



EXTENDED GENOME REPORT

Open Access



# The complete genome sequence and emendation of the hyperthermophilic, obligate iron-reducing archaeon “*Geoglobus ahangari*” strain 234<sup>T</sup>

Michael P. Manzella<sup>1</sup>, Dawn E. Holmes<sup>2</sup>, Jessica M. Rocheleau<sup>2</sup>, Amanda Chung<sup>2</sup>, Gemma Reguera<sup>1</sup> and Kazem Kashefi<sup>1\*</sup>

## Abstract

“*Geoglobus ahangari*” strain 234<sup>T</sup> is an obligate Fe(III)-reducing member of the *Archaeoglobales*, within the archaeal phylum *Euryarchaeota*, isolated from the Guaymas Basin hydrothermal system. It grows optimally at 88 °C by coupling the reduction of Fe(III) oxides to the oxidation of a wide range of compounds, including long-chain fatty acids, and also grows autotrophically with hydrogen and Fe(III). It is the first archaeon reported to use a direct contact mechanism for Fe(III) oxide reduction, relying on a single archaeellum for locomotion, numerous curled extracellular appendages for attachment, and outer-surface heme-containing proteins for electron transfer to the insoluble Fe(III) oxides. Here we describe the annotation of the genome of “*G. ahangari*” strain 234<sup>T</sup> and identify components critical to its versatility in electron donor utilization and obligate Fe(III) respiratory metabolism at high temperatures. The genome comprises a single, circular chromosome of 1,770,093 base pairs containing 2034 protein-coding genes and 52 RNA genes. In addition, emended descriptions of the genus “*Geoglobus*” and species “*G. ahangari*” are described.

**Keywords:** *Euryarchaeota*, *Archaeoglobales*, Hydrothermal vent, Guaymas basin, Fe(III) respiration, Extracellular electron transfer, Autotroph

## Introduction

“*Geoglobus ahangari*” strain 234<sup>T</sup> is the type strain and one of only two known members of the *Geoglobus* genus within the order *Archaeoglobales* and the family *Archaeoglobaceae*. It is an obligate Fe(III)-reducing archaeon isolated from the Guaymas Basin hydrothermal system and grows at temperatures ranging from 65–90 °C, with an optimum at about 88 °C [1]. It was the first isolate in a novel genus within the *Archaeoglobales* and the first example of a dissimilatory Fe(III)-reducer able to grow autotrophically with H<sub>2</sub> [1], a metabolic trait later shown to be conserved in many hyperthermophilic Fe(III) reducers [2]. “*G. ahangari*” can also couple the reduction of soluble and insoluble Fe(III) acceptors to the

oxidation of a wide range of carbon compounds including long-chain fatty acids such as stearate and palmitate, which were previously not known to be used as electron donors by archaea [1]. It was also the first hyperthermophile reported to fully oxidize acetate to CO<sub>2</sub>, a metabolic function once thought to occur solely in mesophilic environments [3]. Unlike the other two genera in the order *Archaeoglobales* (*Archaeoglobus* and *Ferroglobus*), which can utilize acceptors such as sulfate and nitrate [1, 4–10], the two cultured members of the genus *Geoglobus* can only use Fe(III) as an electron acceptor [1, 4]. The obligate nature of Fe(III) respiration in *Geoglobus* spp. makes the genus an attractive model to gain insights into the evolutionary mechanisms that may have led to the loss and/or gain of genes involved in the respiration of iron and other electron acceptors such as sulfur- and nitrogen-containing compounds within the *Archaeoglobales*.

\* Correspondence: kashefi@msu.edu

<sup>1</sup>Department of Microbiology and Molecular Genetics, Michigan State University, East Lansing, MI, USA

Full list of author information is available at the end of the article

“*G. ahangari*” strain 234<sup>T</sup> also serves as a model organism for mechanistic studies of iron reduction at high (>85 °C) temperatures. Dissimilatory Fe(III) reduction has been extensively studied in mesophilic bacteria (reviewed in references [11, 12]). By contrast, little is known about the mechanisms that allow (hyper)thermophilic organisms to respire Fe(III) acceptors [13–18]. As previously observed in the thermophilic Gram-positive bacterium *Carboxydotherrmus ferrireducens* [13], “*G. ahangari*” also needs to directly contact the insoluble Fe(III) oxides to transfer respiratory electrons [14]. In “*G. ahangari*”, cells are motile via a single archaellum, which could help in locating the oxides, and also express numerous curled extracellular appendages, which bind the mineral particles and position them close to heme-containing proteins on the outer surface of the cell to facilitate electron transfer [14]. A direct contact mechanism such as this is predicted to confer on these organisms a competitive advantage over other organisms relying on soluble mediators such as metal chelators [19] and electron shuttles [20, 21], which are energetically expensive to synthesize and are easily diluted or lost in the environment once excreted [22]. This is particularly important in hydrothermal vent systems such as the Guaymas basin chimney where “*G. ahangari*” strain 234<sup>T</sup> was isolated, as vent fluids in these systems can flow through at rates as high as 2 m/s [23]. Here, we report the complete genome sequence of “*G. ahangari*” strain 234<sup>T</sup> and summarize the physiological features

that make this organism a good model system to study Fe(III) reduction in hot environments and to gain insights into the evolution of Fe(III) respiration in the family *Archaeoglobales*.

## Organism information

### Classification and features

“*Geoglobus ahangari*” strain 234<sup>T</sup> is a euryarchaeon originally isolated from samples obtained from a hydrothermal chimney located within the Guaymas Basin (27° N, 111° W) at a depth of 2000 m [1]. The sequence of the single 16S rRNA gene found in its genome was 99 % identical to the previously published 16S rDNA sequence (AF220165). The full length 16S rRNA gene (1485 bp) was used to construct a phylogenetic tree in reference to 16S rRNA gene sequences from other hyperthermophilic archaea using two thermophilic bacteria (“*Aquifex aeolicus*” and *Pseudothermotoga thermarum*) as outgroups (Fig. 1). The closest known relative was *Geoglobus acetivorans* (97 % identical), the only other known member of the *Geoglobus* genus, which also is available in pure culture [4]. Closest relatives outside the genus were other hyperthermophilic archaea within the family *Archaeoglobaceae* such as the sulfate-reducing *Archaeoglobus* species *A. fulgidus* and *A. profundus* (97 and 93 % identical, respectively) and *Ferroglobus placidus* (94 % identical), which can reduce Fe(III), thiosulfate, and nitrate [3, 5].

Cells of “*G. ahangari*” strain 234<sup>T</sup> are regular to irregular cocci, 0.3 to 0.5 μm in diameter, and usually arranged

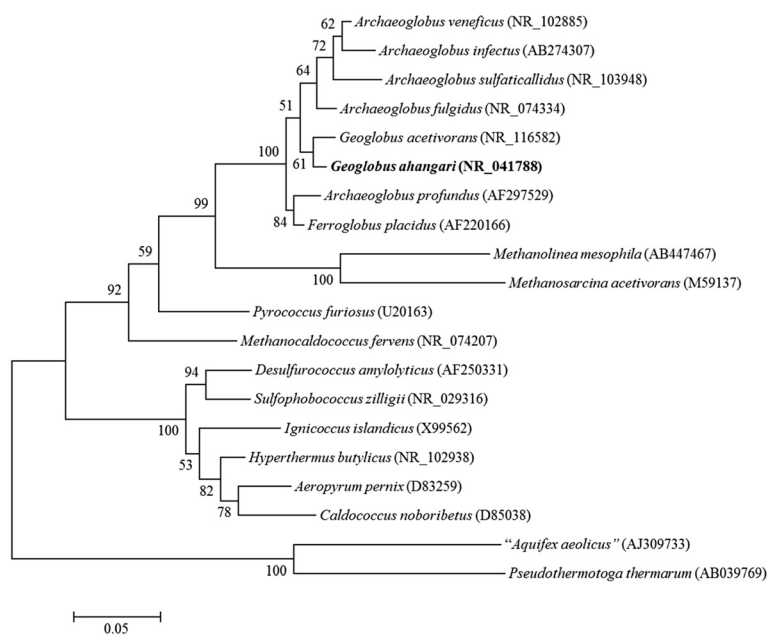


**Fig. 1** Phylogenetic tree. The phylogenetic tree was constructed with the maximum likelihood algorithm comparing the 16S rRNA gene sequence from “*G. ahangari*” to other hyperthermophilic archaea. Bootstrap values were determined from 100 replicates and “*Aquifex aeolicus*” and *Pseudothermotoga thermarum* were used as outgroups

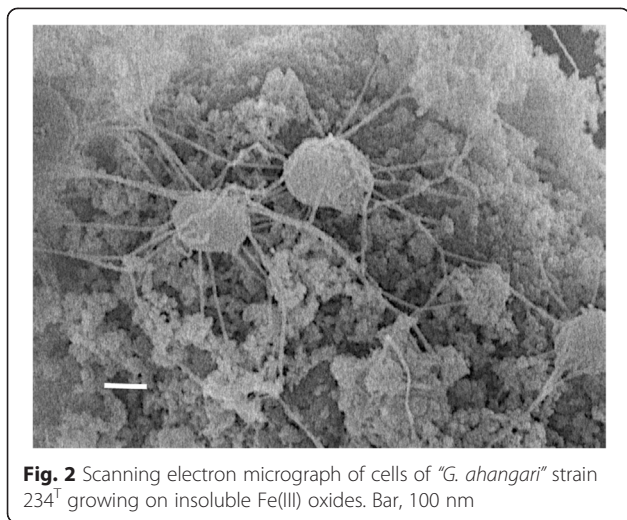


**Fig. 2** Scanning electron micrograph of cells of “*G. ahangari*” strain 234<sup>T</sup> growing on insoluble Fe(III) oxides. Bar, 100 nm

as single cells or in pairs (Fig. 2 and Table 1) [1]. Cells are motile via a single archaeellum [1], but also produce abundant extracellular curled filaments when grown with both soluble and insoluble Fe(III) [14]. Though optimum growth occurs at *ca.* 88 °C, growth is observed between 65 and 90 °C [1]. Furthermore, growth was supported at pH values between 5.0 and 7.6, with an optimum at pH 7.0, and with NaCl concentrations ranging from 9 to 38 g/L, with an optimum at 19 g/L [1].

A distinctive feature of the metabolism of “*G. ahangari*” strain 234<sup>T</sup> is its obligate nature of Fe(III) respiration, with both soluble and insoluble Fe(III) species supporting growth but the insoluble electron acceptor being preferred [1]. The obligate nature of Fe(III) reduction contrasts with the wide range of electron donors that “*G. ahangari*” can oxidize [1]. Acetate, alongside a number of other organic acids (such as propionate, butyrate, and valerate), several amino acids, and both short-chain and long-chain fatty acids were completely oxidized to CO<sub>2</sub> to support growth during Fe(III) respiration [1, 3]. Furthermore, “*G. ahangari*” strain 234<sup>T</sup> was also able to grow autotrophically with H<sub>2</sub> as the sole electron donor and Fe(III) as the electron acceptor [1]. The main physiological features of the organism are listed in Table 1.

## Genome sequencing and annotation

### Genome project history

Based on its unique physiological characteristics [1] and use as a model system for mechanistic investigations of Fe(III) reduction by hyperthermophilic archaea [14], “*G. ahangari*” strain 234<sup>T</sup> was selected for sequencing. Insights from its genome sequence and annotation provide greater understanding of the evolution of

respiratory metabolisms in the *Archaeoglobales*, and, in particular, about hyperthermophilic iron reduction within the *Archaea*. The genome project information is listed in the Genomes OnLine Database (Gp0101274) [24] and the complete genome sequence has been deposited in GenBank (CP011267). A summary of the project information is shown in Table 2.

### Growth conditions and genomic DNA preparation

“*G. ahangari*” strain 234<sup>T</sup> was from our private culture collection and is available at the Deutsche Sammlung von Mikroorganismen und Zellkulturen (*DSM-27542*), the Japan Collection of Microorganisms (*JCM 12378*), and the American Type Culture Collection (*BAA-425*). The strain was grown in marine medium [1] with 10 mM pyruvate as the electron donor and 56 mM ferric citrate as the electron acceptor. Cultures were incubated under a N<sub>2</sub>:CO<sub>2</sub> (80:20 %, v/v) atmosphere at 80 °C or 85 °C in the dark. Strict anaerobic techniques were used throughout the culturing and sampling experiments [25].

gDNA was extracted as previously reported for *F. placidus* [26]. Alternatively, cells were lysed with an SDS-containing lysis buffer (5 % SDS, 0.125 M EDTA, 0.5 M Tris, pH 9.4), as reported elsewhere for the preparation of whole cell extracts from “*G. ahangari*” [14], and gDNA was extracted using the MasterPure™ DNA Purification Kit (EPICENTRE® Biotechnologies), according to the manufacturer suggested guidelines.

### Genome sequencing and assembly

The finished genome of “*G. ahangari*” strain 234<sup>T</sup> (CP 011267) was generated from Illumina [27] draft sequences generated independently at the Research Support and Training Facility at Michigan State University, the Deep Sequencing Core Facility at the University of Massachusetts Medical School, and the Genomics Resource lab at the University of Massachusetts-Amherst. Table 2 presents the project information.

The sequencing project at the University of Massachusetts facilities used gDNA suspended in 3 ml of sonication buffer (4.95 % glycerol, 10 mM Tris–HCl (pH 8.0), 1 mM EDTA) and sonicated for 10 min (2 min on, 30 s off) using a 550 Sonic Dismembrator (Fisher Scientific). The samples were then dispensed as equal volumes into 4 tubes and mixed with 150 µl TE buffer (10 mM Tris–HCl (pH 8.0), 1 mM EDTA), 100 µl ammonium acetate (5 M), 20 µl glycogen (5 mg/ml), and 1 ml of cold (–20 °C) isopropanol. Nucleic acids were precipitated at –30 °C for 1 h, as previously described [26] and suspended in EB buffer (Qiagen) before separating the DNA fragments in the sample by agarose gel electrophoresis. DNA fragments between 300–500 bp were then purified with the QiaQuick Gel Extraction Kit (Qiagen). All steps involved in end repair, 3' adenylation, adaptor ligation, and purification of

**Table 1** Classification and general features of “*G. ahangari*” 234<sup>T</sup> according to the MIGS recommendations [106]

| MIGS ID  | Property               | Term   | Evidence code <sup>a</sup> |
|----------|------------------------|--|----------------------------|
|          | Current classification | Domain <i>Archaea</i>  | TAS [107]                  |
|          |                        | Phylum <i>Euryarchaeota</i>                                  | TAS [107, 108]             |
|          |                        | Class <i>Archaeoglobi</i>                                    | TAS [109]                  |
|          |                        | Order <i>Archaeoglobales</i>                                 | TAS [110]                  |
|          |                        | Family <i>Archaeoglobaceae</i>                               | TAS [111]                  |
|          |                        | Genus <i>Geoglobus</i>                                       | TAS [1]                    |
|          |                        | Species “ <i>Geoglobus ahangari</i> ”                        | TAS [1]                    |
|          |                        | Type strain 234 <sup>T</sup>                                 | TAS [1]                    |
|          |                        | Gram stain   | Variable                   |
|          | Cell shape             | Irregular coccus   | TAS [1]                    |
|          | Motility               | Motile   | TAS [1]                    |
|          | Sporulation            | Non-sporulating  | NAS                        |
|          | Temperature range      | 65–90 °C   | TAS [1]                    |
|          | Optimal temperature    | 88 °C  | TAS [1]                    |
|          | pH range; Optimum      | 5.0–7.6 (optimum 7.0)  | TAS [1]                    |
|          | Carbon source          | CO <sub>2</sub>  | TAS [1]                    |
|          | Energy metabolism      | Chemolithoautotrophic, chemolithotrophic, chemoorganotrophic | TAS [1]                    |
| MIGS-6   | Habitat                | Marine geothermally heated areas                             | TAS [1]                    |
| MIGS-6.3 | Salinity               | 9.0–38 g/L NaCl  | TAS [1]                    |
| MIGS-22  | Oxygen requirement     | Anaerobe   | TAS [1]                    |
| MIGS-15  | Biotopic relationship  | Free-living  | TAS [1]                    |
| MIGS-14  | Pathogenicity          | Non-pathogen   | NAS                        |
|          | Isolation              | Hydrothermal vent chimney                                    | TAS [1]                    |
| MIGS-4   | Geographic location    | Guaymas Basin hydrothermal system                            | TAS [1]                    |
| MIGS-5   | Sample collection time | Unknown  | NAS                        |
| MIGS-4.1 | Latitude               | 27° N  | TAS [1]                    |
| MIGS-4.2 | Longitude              | 111° W   | TAS [1]                    |
| MIGS-4.3 | Depth                  | 2000 m   | TAS [1]                    |
| MIGS-4.4 | Altitude               | Not applicable   |                            |

<sup>a</sup>Evidence codes – *IDA* Inferred from Direct Assay, *TAS* Traceable Author Statement (i.e., a direct report exists in the literature), *NAS* Non-traceable Author Statement (i.e., not directly observed for the living, isolated sample, but based on a generally accepted property for the species, or anecdotal evidence). These evidence codes are from the Gene Ontology project [112]

Illumina products were performed using reagents supplied by the TruSeq DNA Sample Prep Kit (Illumina). This resulted in the construction and sequencing of five independent 100 bp paired-end Illumina shotgun libraries which generated 7,970,036, 7,970,182, 7,973,896, 7,966,671 and 3,144,785 reads totaling 3.50 Gbp. The Illumina draft sequences were assembled *de novo* with SeqMan NGen (DNASTAR) and Velvet [28] (version 1.2.10) and optimized with VelvetOptimiser (version

2.2.5). Reads were down-sampled to 500x coverage to increase the efficacy of the Velvet assembler while the complete depth of reads was used to verify the final genome assembly.

A total of 1,780,565 bp were assembled into 25 scaffolds ranging in size from 207 bp to 510,180 bp. The scaffolds were then connected by adaptor-PCR as previously described [29]. “*G. ahangari*” gDNA was subsequently digested separately by four different restriction

**Table 2** Genome sequencing project information

| MIGS ID   | Property                   | Term  |
|-----------|----------------------------|---|
| MIGS-31   | Finishing quality          | Finished  |
| MIGS-28   | Libraries used             | 5 independent 100 bp paired-end Illumina shotgun libraries, 150 bp paired-end Illumina shotgun library                                |
| MIGS-29   | Sequencing platforms       | Illumina MiSeq  |
| MIGS-31.2 | Sequencing coverage        | 1,977 × coverage (100 bp libraries)<br>100 × (150 bp library)   |
| MIGS-30   | Assemblers                 | SeqMan NGen, Velvet, SeqMan Pro   |
| MIGS-32   | Gene calling method        | JGI-ER, GLIMMER   |
|           | INSDC ID                   | CP011267  |
|           | Genbank Date of Release    | May 11, 2015  |
|           | GOLD ID                    | Gp0101274   |
|           | NCBI project ID            | 258102  |
| MIGS-13   | Source material identifier | ATCC BAA-425, DSMZ DSM-27542, JCM JCM 12378   |
|           | Project relevance          | Phylogenetic diversity, biotechnology, evolution of metal respiration in hyperthermophiles, and anaerobic degradation of hydrocarbons |

enzymes (*EcoRI*, *BamHI*, *BclI*, and *Sall*). After a 1.5-h incubation at 37 °C (or 50 °C for *Sall*), the restriction digests were separated by agarose gel electrophoresis and fragments between 5–10 kb were isolated and purified with the QiaQuick gel extraction kit (Qiagen). Adaptor sequences with 3' overhangs generated by *EcoRI*, *BamHI*, *BclI*, and *Sall* at the phosphorylated 5' ends were then ligated with T4 DNA ligase to the fragments purified from the restriction digests of "*G. ahangari*" gDNA. The adaptor sequences used were: *EcoRI* adaptor AATCCCC TATAGTGAGTCGTATTAAC\*\* (phosphorylated at 5' end); *BclI* and *BamHI* adaptor GATCCCCCTATAGTGAG TCGTATTAAC\*\*; and finally the *Sall* adaptor TCGACCC TATAGTGAGTCGTATTAAC\*\*. Further assembly was performed with SeqMan Pro (DNASTAR) and primers were designed targeting the 3' and 5' ends of the 25 scaffolds. The adaptor ligations were diluted 100-fold and 1 µl of the diluted sample was used in PCR reactions with AccuTaq™ LA DNA Polymerase (50 µl total volume) according to manufacturer specifications (Sigma-Aldrich). Fifty reactions were performed with "*G. ahangari*"-specific primers designed from the various Illumina scaffolds and a non-phosphorylated primer that complemented the adaptor sequence on the gDNA (GTTAATACGACTCAC TATAGGG). All PCR products were purified with the

Qiagen PCR purification kit and sent for sequencing at the University of Massachusetts (Amherst) sequencing facility. This process was repeated until a single contig was obtained using SeqMan Pro assembly software.

The assembly was then verified against a second, independent genome assembly generated at Michigan State University. Extracted gDNA was used to construct a single Illumina shotgun library using the Illumina DNAseq Library Kit, which was sequenced in two 150 bp paired-end runs with an Illumina MiSeq at the Research Support and Training Facility at Michigan State University. The sequencing project generated 1,233,811 and 796,056 reads totaling 304.5 Mbp. Reads were quality trimmed using a combination of fastq-mcf [30] (ea-utils.1.1.2-537, using default parameters) and ConDeTri [31] (v2.2, using default parameters with the exception of hq = 33 and sc = 33) to remove low-quality reads and over-represented sequences. High-quality paired and unpaired reads were assembled using Velvet [28] (v1.2.08 using default parameters and a kmer value of 63) to generate a new assembly (1.77 Mbp, 51 contigs ≥ 1000 bp, and an N75 of 37,520 bp). The second assembly was then compared to the primary assembly to identify errors and low-coverage regions, which were subsequently resolved by PCR-amplifying and sequencing the regions of interest.

### Genome annotation

Initial genome annotation was performed by the RAST server [32], the IGS Annotation Engine [33] at the University Of Maryland School Of Medicine, and the IMG-ER platform [34]. The annotations were compared to manual annotations performed using GLIMMER [35] for gene calls and DELTA-BLAST analysis to identify conserved domains and homology to known proteins. EC numbers and COG categories were determined with a combination of DELTA-BLAST analysis of each annotated gene and the IMG-ER platform. Pseudogenes were identified using the GenePRIMP pipeline [36]. The data were used to create a consensus annotation before the final assembled genome was uploaded onto the IMG-ER platform. IMG-ER annotations were manually curated by comparison to the consensus annotation before submitting the final genome annotation.

Potential *c*-type cytochromes were selected based on the presence of *c*-type heme binding motifs (CXXCH) within the amino acid sequence as previously described [37]. Predicted subcellular localization and the presence of signal peptides and/or an N-terminal membrane helix anchor [37] was investigated by PsortB [38], PRED-TAT [39], TMPred [40], and the TMHMM Server (v. 2.0) [41]. Putative *c*-type cytochromes were then examined by BLAST analysis to determine homology to known *c*-type cytochromes in the NCBI database. The molecular

weight of putative *c*-type cytochromes was estimated with the ExPASy ProtParam program [42]. The weight of the signal peptide was then subtracted from the predicted weight and 685 daltons were added for each heme-binding motif to estimate the molecular weight of the mature cytochrome. The predicted molecular weight values and subcellular localization of the mature cytochromes were compared to the masses reported for mature heme-containing proteins present in whole cells and outer-surface protein preparations of “*G. ahangari*” [14].

### Genome properties

The genome of “*G. ahangari*” strain 234<sup>T</sup> comprises one circular chromosome with a total size of 1,770,093 bp and does not contain any plasmids. The genome size is within the range of those reported for other members of the *Archaeoglobales* [15, 26, 43–45], and NC\_015320.1. The mol percent G + C is 53.1 %, which is lower than the 58.7 % estimated experimentally via HPLC [1]. Out of the total 2072 genes annotated in the genome, 52 were identified as RNA genes and 2020 as protein-coding genes (Table 3). There are 47 pseudogenes, comprising 2.3 % of the protein-coding genes. Furthermore, 76.5 % of the predicted genes (1557) are represented by COG functional categories. Distribution of these genes

**Table 3** Nucleotide content and gene count levels of the genome

| Attribute                        | Value     | % of total <sup>a</sup> |
|----------------------------------|-----------|-------------------------|
| Size (bp)                        | 1,770,093 | 100.0 %                 |
| Coding region (bp)               | 1,662,832 | 93.9 %                  |
| G + C content (bp)               | 940,071   | 53.1 %                  |
| Number of replicons              | 1         |                         |
| Extrachromosomal elements        | 0         |                         |
| Total genes                      | 2072      | 100.0 %                 |
| RNA genes                        | 52        | 2.5 %                   |
| rRNA operons                     | 2         |                         |
| Protein-coding genes             | 2034      | 100.0 %                 |
| Pseudogenes                      | 47        | 2.3 %                   |
| Genes with function prediction   | 1677      | 82.4 %                  |
| Genes in paralog clusters        | 1406      | 69.1 %                  |
| Genes assigned to COGs           | 1470      | 72.2 %                  |
| Genes assigned Pfam domains      | 1667      | 82.0 %                  |
| Genes with signal peptides       | 55        | 2.7 %                   |
| Genes with transmembrane helices | 409       | 20.1 %                  |
| CRISPR repeats                   | 7         |                         |

<sup>a</sup>The total is based on either the size of the genome in base pairs or the total number of protein coding genes in the annotated genome

and their percentage representation are listed in Fig. 3 and Table 4.

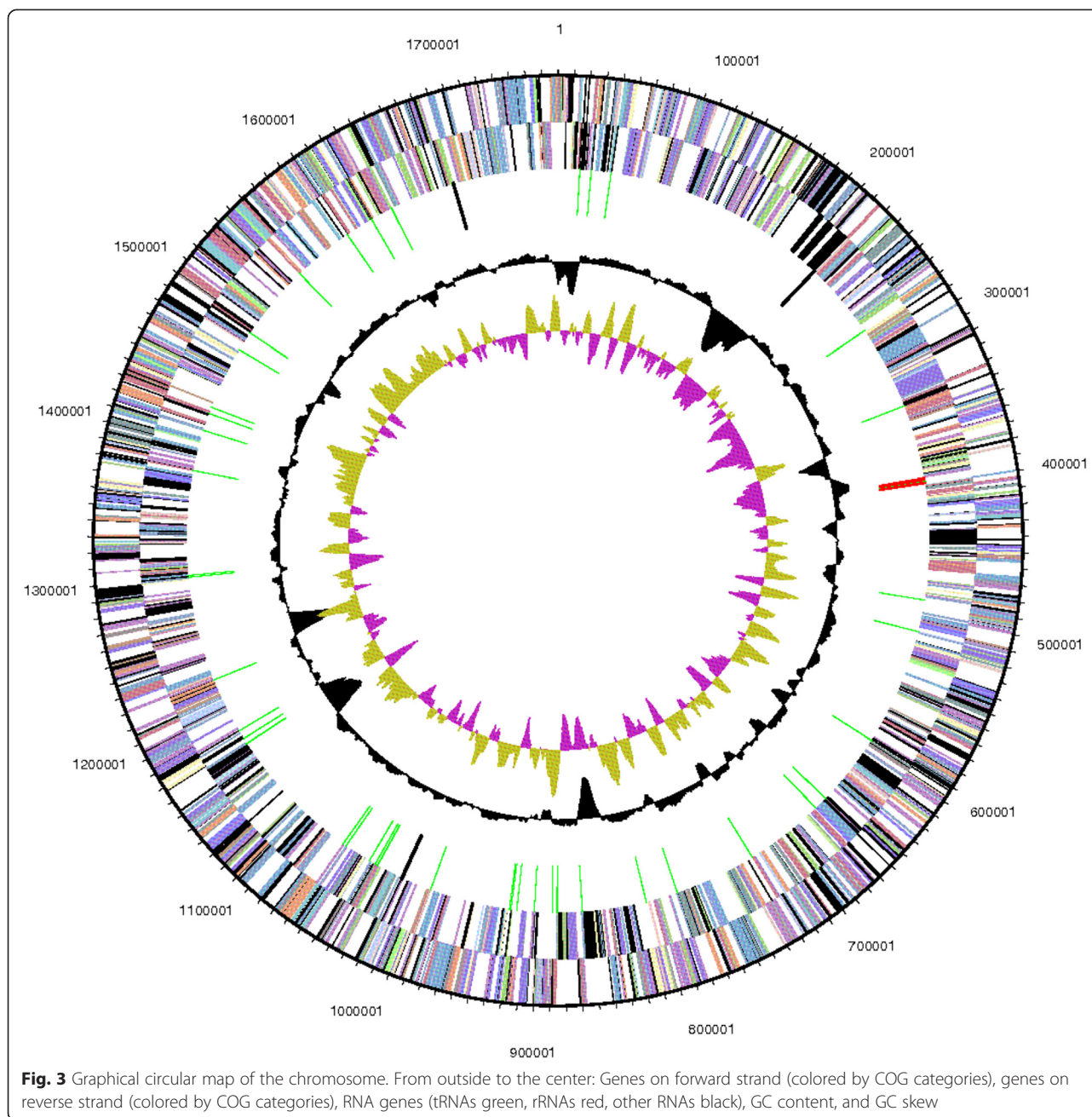
The preferred start codon is ATG (83.8 % of the genes), followed by GTG (10.4 %) and TTG (5.7 %). This distribution is similar to the start codon representation of the other member of the *Geoglobus* genus, *G. acetivorans* (79.4 % ATG, 11.6 % GTG, and 9.0 % TTG) [15] and the closely related archaeon *F. placidus* (82.5 % ATG, 10.2 % GTG, 6.1 % TTG, and 1.3 % other) [26]. There is one copy of each of the rRNA genes but the genes are located in two different regions of the genome: the 16S rRNA (GAH\_00462) and 23S rRNA (GAH\_00460) genes are in the same gene cluster and separated by a span of 139 bp encoding a single tRNA whereas the 5S rRNA (GAH\_02069) is located 205,273 bp away in a region with genes coding for proteins with functions unrelated to ribosome function and biogenesis.

Almost all origins of DNA replication identified in *Archaea* to date are located in close proximity to genes coding for a homologue of the eukaryotic Cdc6 and Orc1 proteins [46]. Interestingly, we identified two genes encoding Orc1/Cdc6 family replication initiation proteins (GAH\_00094 and GAH\_00965) in the genome of “*G. ahangari*”, thus raising the possibility that the genome contains more than one functional origin of replication. Many archaeal replication origins consist of long intergenic sequences upstream of the *cdc6* gene containing an A/T-rich duplex unwinding element flanked by several conserved repeat motifs known as ORBs [47]. A specific ORB could not be identified in the genome when compared to other archaeal origins of replication available in the DoriC database [48]. However, the 320-bp long region upstream of GAH\_00965, one of the Orc1/Cdc6 family replication initiation proteins, contains a long (111 bp) non-coding intergenic region with one AT-rich stretch and 8 direct repeats (3 TCGTGG, 3 CGTGGTC, and 2 GGGGATTA), which could function as a replication origin. Furthermore, the 580-bp region directly upstream of the other Orc1/Cdc6 family replication initiation protein (GAH\_00094) lacks a non-coding intergenic region and/or AT-rich span but contains 8 direct repeats (2 GGTTGAGAAG, 3 TGAGAAG, and 3 AACATCCCG) and several “G-string” elements analogous to *ori* sites reported for haloarchaeal species [49].

### Insights from the genome

#### Autotrophic growth with H<sub>2</sub> as electron donor

“*G. ahangari*” strain 234<sup>T</sup> was the first dissimilatory Fe (III)-reducing hyperthermophile shown to grow autotrophically with H<sub>2</sub> as an electron donor [1]. In its genome, we identified genes required for the two branches of the reductive acetyl-CoA/Wood-Ljungdahl pathway [50–53], which other members of the Euryarchaeota [54], including most members of the *Archaeoglobales* [8, 45, 55–58],



use for carbon fixation. A bifunctional carbon monoxide dehydrogenase/acetyl-CoA synthase complex (encoded by GAH\_01139-01144, and two additional copies of the beta and maturation factors encoded by GAH\_00919 and GAH\_00306, respectively) are present within the genome, which could initiate carbon fixation. The bifunctional nature of this enzyme also allows it to link methyl and carbonyl branches and enable acetyl-CoA biosynthesis, as reported for methanogenic archaea [59]. Complete enzymatic pathways for alternative means of carbon fixation were not identified.

The genome of "*G. ahangari*" also contains 29 genes encoding hydrogenase subunits, maturation proteins, and a cluster of genes (*hypA*, *hypB*, *hypC*, *hypD*, and *hypE*) involved in biosynthesis and assembly of Ni-Fe hydrogenases (GAH\_00190-00195). Genes coding for the large, small, and *b*-type cytochrome subunits of a Ni-Fe hydrogenase I protein (GAH\_00910-00912) were identified in the genome. We also found a gene cluster (GAH\_00337-00347) encoding all subunits of a NADH-quinone oxidoreductase, which transfers electrons to the quinone membrane pool and may function as the

**Table 4** Number of genes associated with the 25 general COG functional categories

| Code | Value | % age <sup>a</sup> | Description  |
|------|-------|--------------------|--|
| J    | 155   | 7.6 %              | Translation, ribosomal structure and biogenesis              |
| A    | 2     | 0.1 %              | RNA processing and modification                              |
| K    | 68    | 3.3 %              | Transcription  |
| L    | 58    | 2.9 %              | Replication, recombination and repair                        |
| B    | 6     | 0.3 %              | Chromatin structure and dynamics                             |
| D    | 20    | 1.0 %              | Cell cycle control, Cell division, chromosome partitioning   |
| Y    | 0     | 0.0 %              | Nuclear structure  |
| V    | 7     | 0.3 %              | Defense mechanisms   |
| T    | 24    | 1.2 %              | Signal transduction mechanisms                               |
| M    | 35    | 1.7 %              | Cell wall/membrane biogenesis                                |
| N    | 15    | 0.7 %              | Cell motility  |
| Z    | 0     | 0.0 %              | Cytoskeleton   |
| W    | 0     | 0.0 %              | Extracellular structures                                     |
| U    | 23    | 1.1 %              | Intracellular trafficking and secretion                      |
| O    | 57    | 2.8 %              | Posttranslational modification, protein turnover, chaperones |
| C    | 160   | 7.9 %              | Energy production and conversion                             |
| G    | 37    | 1.8 %              | Carbohydrate transport and metabolism                        |
| E    | 139   | 6.8 %              | Amino acid transport and metabolism                          |
| F    | 49    | 2.4 %              | Nucleotide transport and metabolism                          |
| H    | 103   | 5.1 %              | Coenzyme transport and metabolism                            |
| I    | 55    | 2.7 %              | Lipid transport and metabolism                               |
| P    | 86    | 4.2 %              | Inorganic ion transport and metabolism                       |
| Q    | 16    | 0.8 %              | Secondary metabolites biosynthesis, transport and catabolism |
| R    | 244   | 12.0 %             | General function prediction only                             |
| S    | 198   | 9.7 %              | Function unknown   |
| -    | 477   | 23.5 %             | Not in COGs  |

<sup>a</sup>The total is based on the total number of protein coding genes in the genome

primary generator of the proton-motive force [43]. Another large cluster of hydrogenase genes (GAH\_02036-02044) codes for all coenzyme  $F_{420}$  hydrogenase subunits and proteins involved in recycling coenzyme  $F_{420}$ , thus replenishing the cofactor for the reductive acetyl-CoA pathway [58, 60–62]. The presence of multiple hydrogenases is not unusual in iron-reducing microorganisms and allows them to diversify the paths used to transfer electrons derived from the oxidation of  $H_2$  to their acceptors [63].

Autotrophic growth in methanogens can also be supported using reduced coenzyme  $F_{420}$  as an electron donor to produce methane [64]. The distinctive fluorescence emission from this coenzyme has been detected

in members of the *Archaeoglobales* [7–9, 55, 57] but not in the iron-respiring *F. placidus* [5] or in “*G. ahangari*” [1]. Yet, the “*G. ahangari*” genome contains genes for all coenzyme subunits of the proteins coenzyme  $F_{420}$ -reducing hydrogenase (GAH\_00337 and GAH\_02036-02038), coenzyme  $F_{420}$ -dependent  $N^5,N^{10}$ -methylene tetrahydromethanopterin reductase (GAH\_01605, GAH\_01835), and  $F_O$  synthase (CofGH) (GAH\_00662, GAH\_00663) [65]. Furthermore, although “*G. ahangari*” cannot produce methane when growing autotrophically [1], its genome codes for nearly all enzymes responsible for the reduction of  $CO_2$  to methane [51]. Similar to *A. fulgidus*, *F. placidus*, *A. sulfaticallidus*, and *G. acetivorans*, “*G. ahangari*” has genes encoding all proteins involved in

the formation of 5-methyl-tetrahydromethanopterin and a gene coding for one of the 8 subunits (MtrH) of the enzyme responsible for the transfer of a methyl group to coenzyme M (GAH\_01245). Yet, the genome is missing all four genes required for a functional coenzyme M reductase, the enzyme responsible for the final step of methane production by methanogenic archaea [51]. The fact that *Archaeoglobale* genomes have nearly all of the genes involved in methanogenesis and the high level of homology that exists between genes from the reductive acetyl-CoA pathway in both *Archaeoglobales* and the methanogenic archaea suggests that the *Archaeoglobales* may have evolved from a methanogenic archaeon that lost its ability to reduce CO<sub>2</sub> and produce methane over time.

### Central metabolism

Heterotrophic growth in “*G. ahangari*” is supported by a wide range of organic carbon compounds [1], which serve as electron donor for respiration while also providing carbon for assimilation in the central pathways. Similar to other hyperthermophilic archaeal species [66], the “*G. ahangari*” genome contains a modified Embden-Meyherhof-Parnas glycolytic pathway (Fig. 4). The initial step of glycolysis (glucose phosphorylation to glucose 6-phosphate) is carried out by an ATP-dependent archaeal hexokinase (GAH\_00546) belonging to the ROK family of proteins. A gene coding for the phosphoglucose isomerase enzyme, which catalyzes the next reaction in the pathway (interconversion of the aldose in glucose 6-phosphate

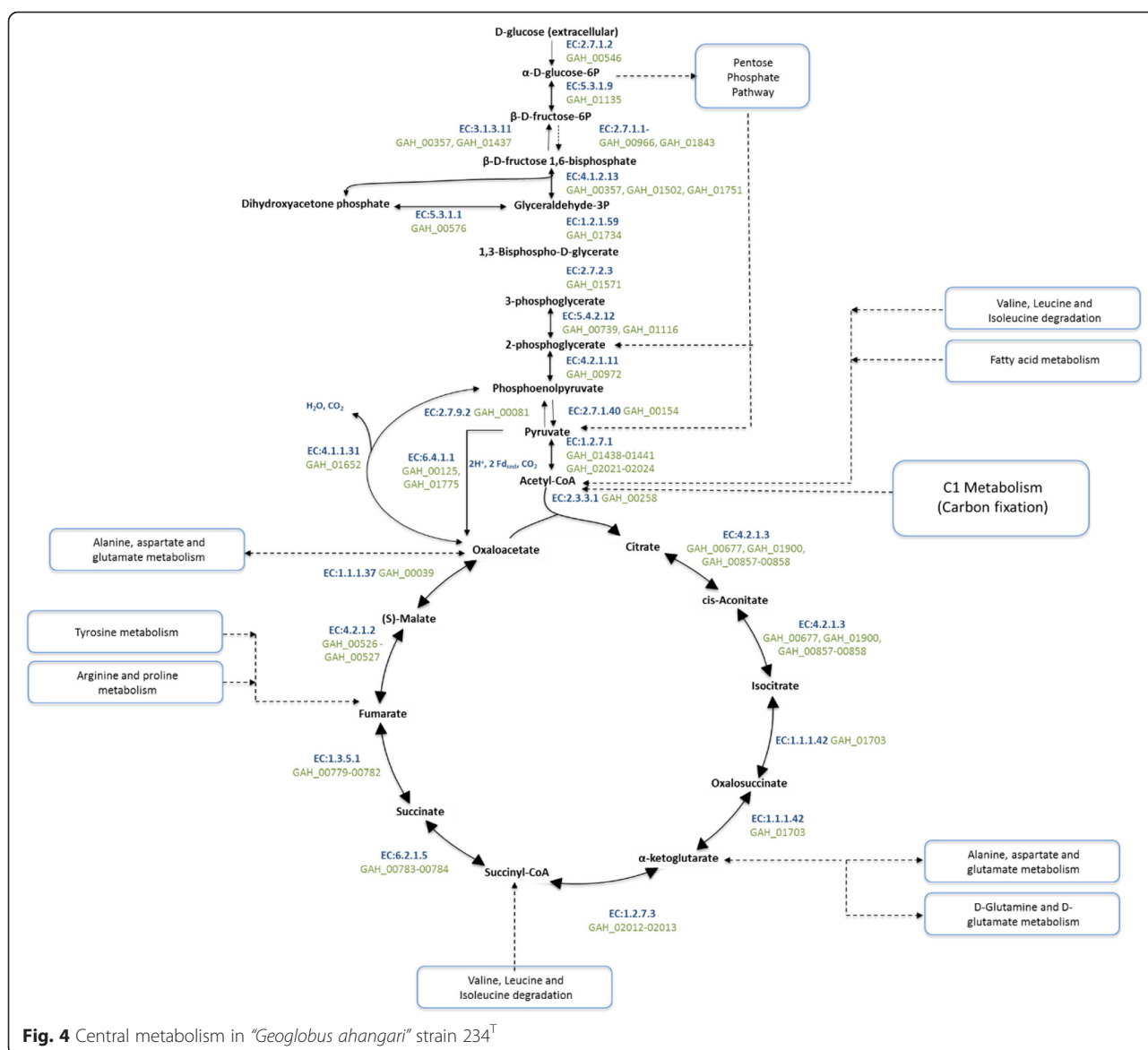


**Fig. 4** Central metabolism in “*Geoglobus ahangari*” strain 234<sup>T</sup>

and the ketose in fructose 6-phosphate) was also identified (GAH\_01135) and was most similar to cupin-type phosphoglucose isomerases from other anaerobic Euryarchaeota, including *Archaeoglobus fulgidus* [66].

In *A. fulgidus*, fructose 6-phosphate is phosphorylated to fructose 1,6-bisphosphate by an ADP-dependent phosphofructokinase protein (EC:2.7.1.11) [67]. However, homologs of this enzyme were not present in the genomes of “*G. ahangari*” or any other *Archaeoglobale* species sequenced to date. Instead, the genome of “*G. ahangari*” contained two genes (GAH\_00966 and GAH\_01843) coding for proteins with pfkB-like domains and ATP-binding sites, which are consistent with the ATP-dependent phosphofructokinases (PFK-B) of other hyperthermophilic archaea such as *Aeropyrum pernix* and *Desulfurococcus amylolyticus* [68, 69]. The genome also contains two genes (GAH\_00357 and GAH\_01437) encoding archaeal fructose 1,6-bisphosphatases, which catalyze the reverse reaction during gluconeogenesis but can also supply fructose 1,6-bisphosphate to the glycolytic pathway from dihydroxyacetone phosphate and *D*-glyceraldehyde 3-phosphate [70]. Furthermore, a triosephosphate isomerase (GAH\_00576) was identified in the genome to catalyze the isomerization of dihydroxyacetone phosphate to *D*-glyceraldehyde 3-phosphate. Alternatively, GAH\_01502 and GAH\_01751, which encode proteins homologous to archaeal type class I fructose 1,6-bisphosphate aldolase proteins, could catalyze the conversion of fructose 1,6-bisphosphate into *D*-glyceraldehyde 3-phosphate.

The next steps in the pathway involve the oxidation of *D*-glyceraldehyde 3-phosphate and formation of 3-phosphoglycerate. The “*G. ahangari*” genome contains a homolog (GAH\_00413) of a GAPOR, which in *A. fulgidus* and many other archaeal species catalyzes the irreversible oxidation of *D*-glyceraldehyde-3-phosphate to 3-phospho-*D*-glycerate bypassing the formation of the intermediate 1,3-bisphospho-*D*-glycerate [66]. In addition, the genome of “*G. ahangari*” contains genes coding for an archaeal specific type II glyceraldehyde-3-phosphate dehydrogenase (GAH\_01734) and a phosphoglycerate kinase (GAH\_01571), which could catalyze the formation of 3-phosphoglycerate via the 1,3-diphosphoglycerate intermediate. These two enzymes are unidirectional and involved in formation of glyceraldehyde-3-phosphate from 3-phosphoglycerate during gluconeogenesis in most hyperthermophilic archaea [66].

As in *A. fulgidus* [71], “*G. ahangari*” has 2 genes coding for cofactor-independent phosphoglycerate mutase proteins (GAH\_00739 and GAH\_01116), which can catalyze the interconversion of 3-phospho-*D*-glycerate to 2-phospho-*D*-glycerate. Phosphoenolpyruvate is then formed by an enolase protein (GAH\_00972), which is subsequently dephosphorylated to pyruvate by pyruvate kinase. Although a gene coding for the well-characterized pyruvate

kinase protein is present in the close relative *F. placidus* (Ferp\_0744), homologs were not identified in “*G. ahangari*” or any other *Archaeoglobale* species. Instead, the genomes of “*G. ahangari*” (GAH\_00154) and all other sequenced *Archaeoglobales* species contain genes encoding PK\_C superfamily proteins [15, 33, 50–52, and NC\_015320.1], which have pyruvate kinase and alpha/beta domains and are homologous to an *A. fulgidus* enzyme with pyruvate kinase activity *in vitro* [72]. Pyruvate can then be converted into acetyl-CoA via pyruvate synthase (GAH\_01438-01441 and GAH\_02021-02024).

As in the close relative *F. placidus* [26], “*G. ahangari*” lacks genes from the oxidative pentose phosphate pathway but is predicted to circumvent this limitation [73] via the use of a complete RuMP pathway (GAH\_00051 and GAH\_01859). The latter results in the accumulation of formaldehyde [73], which in “*G. ahangari*” could be removed by formaldehyde-activating enzymes (GAH\_00575 and GAH\_00673). Ribulose 5-phosphate formed in the RuMP pathway could then be converted into ribose-5-phosphate by a ribose 5-phosphate isomerase and then into PRPP by ribose-phosphate pyrophosphokinase enzymes (GAH\_00743 and GAH\_00557). This supplies PRPP to various anabolic pathways such as the biosynthesis of histidine and purine/pyrimidine nucleotides.

Similar to other *Archaeoglobale* species, a complete TCA cycle is present within the “*G. ahangari*” All enzymes involved in the formation of oxaloacetate from acetyl-CoA (GAH\_00258, GAH\_01703, GAH\_01110, GAH\_02012-02013, GAH\_00784-00784, GAH\_00779-00782, GAH\_00526-00527, and GAH\_00039), including putative aconitase proteins (GAH\_00857-00858) [74], were identified in the genome. Also present is a phosphoenolpyruvate carboxylase (GAH\_01652), which could catalyze the reversible carboxylation of phosphoenolpyruvate to oxaloacetate, a precursor metabolite of many amino acids.

#### Fatty acids as electron donors

“*G. ahangari*” strain 234<sup>T</sup> was the first hyperthermophile reported to completely oxidize long-chain fatty acids anaerobically, an unsuspected capability of hyperthermophilic microorganisms prior to this discovery [1]. Long-chain fatty acids are abundant in sedimentary environments where they accumulate as byproducts of the hydrolysis of complex organic matter and the anaerobic degradation of alkanes [75, 76]. Long-chain fatty acids are also major components of crude oil [77], which is often present in environments inhabited by *Archaeoglobale* species [78]. Consistent with the ability of *Archaeoglobale* members to oxidize long-chain fatty acids, the genomes of “*G. ahangari*” and other members of the *Archaeoglobales* (*F. placidus*, *G. acetivorans*, *A. fulgidus*, and others) contain a large number of genes coding for  $\beta$ -oxidation

pathway enzymes [15, 26, 43]. The *A. fulgidus* genome, for example, contains 57 genes encoding the 5 core proteins (discussed below) involved in  $\beta$ -oxidation [43]. All of these genes were used as BLAST queries against the genomes of *F. placidus* [26], *G. acetivorans* [15], and “*G. ahangari*” and identified 39 homologous proteins in the genomes of the *F. placidus* and *G. acetivorans* and 32 in the genome of “*G. ahangari*”.

Fatty acid degradation in the *Archaeoglobales* is thought to occur in a manner similar to bacteria and mitochondria [43], with the initial step involving activation of a long chain fatty acid to a fatty acyl CoA by a fatty acyl CoA synthetase/ligase. We identified seven genes in “*G. ahangari*” coding for fatty acid CoA synthetase proteins (GAH\_00420, GAH\_00623, GAH\_01111, GAH\_01124, GAH\_01769, GAH\_01899, and GAH\_02051). The next step in the pathway involves the oxidation of the fatty acyl-CoA to a trans-2-enoyl-CoA by acyl-CoA dehydrogenase proteins, which in “*G. ahangari*” are putatively encoded by 11 genes (GAH\_00179, GAH\_00421, GAH\_00484, GAH\_00591, GAH\_01331, GAH\_01442, GAH\_01601, GAH\_01810, and GAH\_02050). A water molecule is then added to trans-2-enoyl-CoA to form (3S)-3-hydroxyacyl-CoA in a reaction catalyzed by an enoyl-CoA hydratase, which in “*G. ahangari*” could be encoded by 4 genes (GAH\_00487, GAH\_00802, GAH\_01332, and GAH\_01602). Two of these genes (GAH\_00487 and GAH\_01602) are in fact hybrid proteins containing an enoyl-CoA hydratase domain fused to a 3-hydroxyacyl-CoA dehydrogenase domain. Hybrid enoyl-CoA hydratase/dehydrogenase proteins such as these have been identified in other archaeal species including the *Archaeoglobales* species *G. acetivorans*, *F. placidus*, and *A. fulgidus* [15, 26, 43].

The next step in the  $\beta$ -oxidation pathway leads to the formation of 3-oxoacyl-CoA in an oxidation reaction that generates NADH and is catalyzed by a 3-hydroxyl-CoA dehydrogenase protein, which in “*G. ahangari*” is likely encoded by several genes (GAH\_00328, GAH\_00487, GAH\_01600, GAH\_01602 – again noting the hybrid nature of GAH\_00487 and GAH\_01602). Finally, acetyl-CoA is removed from the 3-oxo-acyl-CoA molecule by an acetyl-CoA acetyltransferase and is free to enter the TCA cycle. There are 8 genes in the “*G. ahangari*” genome that could catalyze this reaction (GAH\_00292, GAH\_00485, GAH\_00625, GAH\_00626, GAH\_01327, GAH\_01328, GAH\_01886, and GAH\_02049). Additional proteins involved in fatty-acid metabolism include the alpha (GAH\_01318) and beta (GAH\_01319) subunits of a 3-oxoacid CoA-transferase. The large number of genes dedicated to  $\beta$ -oxidation in “*G. ahangari*” and other species within the *Archaeoglobales* provides genomic evidence supporting the notion that long- and short-chain fatty acid oxidation is a conserved metabolic feature within the family.

### Degradation of aromatic compounds and n-alkanes

*F. placidus*, a member of the *Archaeoglobales* closely related to “*G. ahangari*”, can couple the complete oxidation of aromatic hydrocarbons to Fe(III) reduction [79–81]. The “*G. ahangari*” genome does not contain any benzoate degradation genes, further supporting the observation that it cannot utilize aromatic compounds as electron donors for growth [1]. Interestingly, *G. acetivorans*, the other member of the *Geoglobus* genus, has homologues of all genes coding for proteins of the benzoyl-CoA ligation pathway present in *F. placidus*, yet as in “*G. ahangari*” growth on aromatic hydrocarbons has not been observed in *G. acetivorans* [4, 15].

Another member of the *Archaeoglobales*, *A. fulgidus*, can also couple the oxidation of n-alkanes and n-alkenes with sulfur respiration [82, 83]. This archaeon uses an alkylsuccinate synthase and an activating protein (AssD/BssD; AF1449-1450) to oxidize saturated hydrocarbons (n-alkanes in the range of C<sub>10</sub>-C<sub>21</sub>) [83]. We identified homologs of both of these proteins in the genome of “*G. ahangari*” (GAH\_01645-01646) and *G. acetivorans* (Gace\_0420-0421). *A. fulgidus* can also oxidize long chain n-alk-1-enes (C<sub>12:1</sub> to C<sub>21:1</sub>) when thiosulfate is provided as the terminal electron acceptor [82]. Although enzymes involved in the activation of alkenes by *A. fulgidus* have not been characterized, the genome of *A. fulgidus* contains a homologue of a Mo-Fe-S containing enzyme (AF0173-AF0176) [82], which in *Azoarcus* sp. *EBN1* anaerobically hydroxylates a branched alkene [84]. The Mo-Fe-S enzyme consists of 4 subunits including a chaperonin-like protein, a membrane anchor heme-*b* binding subunit, an Fe-S binding subunit, and a molybdopterin-binding subunit [85]. This gene cluster was identified in the genomes of “*G. ahangari*” (GAH\_01285-01288) and *F. placidus* (Ferp\_0121-0123), but not in the other member of the *Geoglobus* genus, *G. acetivorans*.

### Nitrogen compounds as electron acceptors

Except for *F. placidus* [5, 57], all of the *Archaeoglobales*, including “*G. ahangari*” [1], are unable to use nitrate or nitrite as electron acceptors for respiration [4, 6–10] (Table 5). Yet, surprisingly, the genome of “*G. ahangari*” contains several 4Fe-4S domain-containing nitrate and sulfite reductase proteins (GAH\_01242 and GAH\_02063)

**Table 5** Terminal electron acceptors in the *Archaeoglobales*

| Organism                    | Electron acceptors |         |             |         |         |
|-----------------------------|--------------------|---------|-------------|---------|---------|
|                             | Sulfate            | Sulfite | Thiosulfate | Nitrate | Fe(III) |
| <i>Geoglobus</i> spp.       | -                  | -       | -           | -       | +       |
| <i>Ferroglobus placidus</i> | -                  | -       | +           | +       | +       |
| <i>Archaeoglobus</i> spp.   | +/-                | +       | +           | -       | -       |

as well as all four subunits (NarGHIJ) of a nitrate reductase (GAH\_01285-01288). A nitrate/nitrite transporter is also annotated in the genome (GAH\_00501), though it does not cluster with genes involved in nitrate/nitrite respiration and thus may function in the transport of alternative compounds. In addition, we identified a gene in this region of the genome (GAH\_01290) coding for an uncharacterized channel protein, which could potentially function as a nitrate transport protein. The presence of genes encoding both nitrate reductase proteins (NarGHIJ and NirA) combined with the inability of “*G. ahangari*” to use nitrate for respiration [1] suggests a role for these proteins in assimilatory, rather than dissimilatory, nitrate reduction [86].

Similar to *F. placidus*, the “*G. ahangari*” genome does not contain any *nir* or *nrf* genes (for the NADH- and formate-dependent nitrite reductase proteins, respectively), with the exception of several homologues of NirA (GAH\_00501, GAH\_00506, GAH\_01242, and GAH\_02063), a nitrite reductase protein that catalyzes the reduction of nitrite to ammonia and is involved in assimilatory nitrate reduction in other organisms [86]. Also missing are genes coding for nitric and nitrous oxide reductase proteins, which the genome of *F. placidus* contains [26], again supporting the observation that “*G. ahangari*” is not capable of dissimilatory nitrate reduction [1]. The lack of these enzymes helps explain the physiological separation of “*G. ahangari*” from its close phylogenetic relative *F. placidus*, which is capable of dissimilatory nitrate reduction to N<sub>2</sub>O [57]. Furthermore, it is unlikely that the reduction of nitrogen-containing compounds exerts any significant selective pressure on hydrothermal vent microorganisms, as concentrations of these compounds are often low in vent systems [87].

N<sub>2</sub> gas, on the other hand, is the largest reservoir of nitrogen in the ocean [87, 88] and nitrogen fixation supplies hydrothermal vent systems with nitrogen sources for assimilatory growth [87]. Ammonium is particularly abundant in the heavily sedimented Guaymas Basin hydrothermal system [89], from which “*G. ahangari*” was isolated [1], and this could select for organisms with assimilatory rather than dissimilatory nitrogen metabolisms and inhibit nitrogen fixation. Not surprisingly, the annotated genome of “*G. ahangari*” and homology searches for the primary enzymes from the nitrogen fixation pathway (*nifH*, *nifD*, and *nifK*) provided no significant hits, as previously reported for other members of the *Archaeoglobales*.

The genome does contain genes coding for a glutamine synthetase (GAH\_01658), a glutamate synthase (GAH\_01667-01669), and a glutamate dehydrogenase (GAH\_00573 and GAH\_01931). The enzymes glutamine synthetase-glutamate synthase comprise the GS-GOGAT

pathway, and together with the GDH pathway, function as the two major paths for ammonium assimilation in archaea [86]. While the GDH pathway does not use ATP as an energy source, as the GS-GOGAT pathway does, it has a lower affinity for ammonium [86]. The presence of these enzymes and two ammonium transporter proteins (GAH\_00438 and GAH\_01767) for the formation of 2-oxoglutarate and glutamate from ammonium, is consistent with the notion that “*G. ahangari*” is under pressure to assimilate ammonium for anabolic processes.

### Sulfur compounds as electron acceptors

Most members of the *Archaeoglobales* are dissimilatory sulfate-reducing organisms and able to use several sulfur-containing compounds as electron acceptors to fuel their metabolism [5–10] (Table 5). By contrast, “*G. ahangari*” cannot couple the oxidation of electron donors that supported Fe(III) reduction to the respiration of commonly considered sulfur-containing electron acceptors such as sulfate, thiosulfate, sulfite, or S<sup>0</sup> [1]. Interestingly, the genome of “*G. ahangari*” contains two genes (GAH\_02067 and GAH\_01481) coding for sulfate adenylyltransferase, which can initiate the first step in both the dissimilatory and assimilatory sulfate reduction pathways by catalyzing the formation of APS from ATP and inorganic sulfate. The enzyme is also present in the genome of *F. placidus* which, like “*G. ahangari*”, is unable to respire sulfate [5] (Table 5). APS can then be used as substrate in the assimilatory [90–93] or dissimilatory [94, 95] pathway, depending on the needs and capabilities of the microorganism [92]. The assimilatory pathway converts APS to the intermediate PAPS in a reaction catalyzed by an adenylylsulfate kinase, which in “*G. ahangari*” is encoded by GAH\_01478. The genome of “*G. ahangari*” contains genes coding for both the alpha and beta subunits of adenylylsulfate reductase (GAH\_02065-02066), an FAD dependent oxidoreductase protein that reduces APS to sulfite in the dissimilatory pathway. However, the genome lacks genes coding for a dissimilatory sulfite reductase (*dsrAB*), which catalyzes the reduction of sulfite to hydrogen sulfide in the final step of the dissimilatory sulfate reduction pathway [96]. Strong matches could not be found even when the alpha (AAB17213.1) and beta (AEY99618.1) subunits of the sulfite reductase from *A. fulgidus* were used as queries in manual searches.

It is interesting to note that, despite the absence of *dsrAB* genes in the genome, “*G. ahangari*” does have a nitrite and sulfite reductase 4Fe-4S domain-containing protein (GAH\_02063) located in a cluster of genes involved in sulfur metabolism (GAH\_02063-02067). Whether these genes code for functional proteins of the dissimilatory pathway, perhaps with electron donor/acceptor pairs not tested yet, remains to be elucidated. *F. placidus*, for example, has homologs of all of these

genes, except for *dsrAB*, and it grows with thiosulfate as the sole electron acceptor when hydrogen is provided as an electron donor [5]. This capability may be due to the presence of several molybdopterine oxidoreductase proteins within the genome of *F. placidus* that show high similarity to a predicted thiosulfate reductase (NP\_719592.1) from *Shewanella oneidensis*. However, strong homologs of this protein were not present in the genome of “*G. ahangari*”.

#### Fe(III) as the sole electron acceptor for respiration

The most distinctive physiological feature of “*G. ahangari*” strain 234<sup>T</sup> is its dependence on Fe(III) as an electron acceptor for respiration [1]. Both insoluble Fe(III) oxides and soluble species of Fe(III), such as Fe(III) citrate, support growth, though the original isolate did not grow readily with the soluble electron acceptor and required prolonged adaptation under laboratory conditions to grow in its presence [1]. Key to the ability of “*G. ahangari*” to respire the insoluble Fe(III) oxides is the ability of the cells to locate the oxides, attach to them, and position electron carriers of the outer surface close enough to favor the transfer of electrons [14]. Hence, we examined the genome of “*G. ahangari*” for genes that code for cellular components that could be involved in motility and attachment and extracellular electron transfer.

Motility in this organism is enabled by a single flagellum [1], which in archaea is designated as an archaellum to reflect its distinct evolutionary origin [97]. Archaeal flagellar genes can be organized into one of two very well conserved clusters (*fla1* and *fla2*) based on the type and order of genes in the cluster: *flaBC(D/E)FGHIJ* in *fla1* and *flaBGFHIJ* in *fla2* [98]. The *fla1* clusters are exclusively found in *Euryarchaea* while *fla2* clusters are generally associated with the *Crenarchaea*, which includes the *Desulfurococcales* and *Sulfolobales* orders, and are also present within the *Euryarchaeal* order *Archaeoglobales* [98]. Interestingly, the *Archaeoglobales* have members with both types. We identified, for example, a *fla1* gene cluster in the genome of “*G. ahangari*” (GAH\_01994-02001), as in *F. placidus* (Ferp\_1456-1463) [26], while the flagellar genes of *Archaeoglobus* spp. [15, 26, 43–45], and NC\_015320.1 and *G. acetivorans* [15] were of the *fla2* type. It has been suggested that a horizontal gene transfer (HGT) event occurred in the *Ferroglobus* lineage after divergence from the *Archaeoglobus* and *Geoglobus* lineages [15]. Yet, the presence of a *fla1* gene cluster in the flagellated and motile “*G. ahangari*” [1], when compared to the *fla2* gene cluster found in the non-motile and non-flagellated *G. acetivorans* [4], would lend credence to a possible second HGT event within the family.

The genome of “*G. ahangari*” also encodes several glycosyltransferase genes (GAH\_00218, GAH\_00870,

and GAH\_01279) and an oligosaccharyltransferase (GAH\_01455), which could glycosylate the growing archaellum [99] and post-translationally modify surface proteins, as is commonly observed in the *Archaea* [100]. However, chemotaxis proteins, which are present in nearly all sequenced members of the *Archaeoglobales* [15, 26, 43, 44], and NC\_015320.1, with the exception of *A. sulfaticallidus* [45], and are typically found immediately upstream or downstream of the *fla* gene cluster, were absent in “*G. ahangari*”. The lack of chemotaxis genes in “*G. ahangari*” contrasts with their presence in most *Archaeoglobales* genomes, including *G. acetivorans* [15], the other member of the genus. Both *Geoglobus* species were isolated from hydrothermal vent chimneys: *G. acetivorans* from the Ashadze field on the Mid-Atlantic Ridge at a depth of 4100 m [4] and “*G. ahangari*” from a Guaymas Basin chimney at a depth of 2000 m [1]. The hydrothermal fluids spewed from chimneys within the Guaymas Basin system are likely enriched in nutrients after passage through the 300–400 m thick, organic-rich sediments underneath [101]. Furthermore, hydrothermal circulation at this site is high [23], which would rapidly replenish nutrients, both electron donors and fresh Fe(III) oxides, and thus organisms living in this environment may not need to utilize chemotactic mechanisms to seek out these nutrients. By contrast, hydrothermal fluids from offshore spreading systems, such as the Ashadze field, flow through thin sediment layers before reaching the chimney [101]. This likely increases the selective pressure on resident microbes to evolve chemotactic mechanisms to locate nutrients.

The genome of “*G. ahangari*” also encodes proteins potentially involved in the assembly of extracellular protein appendages such as pili. We identified, for example, a prepilin peptidase (GAH\_00760), numerous type II secretion system proteins (GAH\_01195-01196, GAH\_00173, GAH\_00290, GAH\_01412-01413), and a putative twitching motility pilus retraction ATPase (GAH\_00960). Homologous genes are also present in the genomes of *G. acetivorans* [15], *F. placidus* [26], and *A. fulgidus* [43]. In addition, “*G. ahangari*” has two genes encoding proteins with DUF1628 or DUF1628-like domains (GAH\_01202, GAH\_01671), which are associated with previously described archaeal pilin proteins [102] and present in all sequenced members of the *Archaeoglobales* [15, 26, 43–45], and NC\_015320.1. Any of these proteins could be involved in the assembly of the curled extracellular appendages that “*G. ahangari*” produces to attach to Fe(III) oxides and facilitate the transfer of electrons from electron carriers located on the outer surface to the insoluble electron acceptor [14].

“*G. ahangari*” uses heme-containing proteins to transport electrons across the cell envelope and to the insoluble Fe(III) oxides [14]. The most common heme-containing

proteins used by mesophilic Fe(III) reducers for extracellular electron transport are *c*-type cytochromes [103]. Archaea are known to have a variant form of the cytochrome *c* maturation (Ccm) system, whereby the CcmE protein has a CXXXY-type motif, rather than the HXXXY motif found in eukaryotic and most bacterial *c*-cytochromes, and CcmH is absent [37]. Similar to other sequenced *Archaeoglobales*, “*G. ahangari*” has an archaeal-type CcmE protein (GAH\_01977), a CcmC (GAH\_00620) with a tryptophan-rich motif (WG[S,T][F,Y]WNWDPRET), a CcmF protein (GAH\_01976 and GAH\_01093) with the motif WGGXWFWDPVEN, and a gene coding for a CcmB homolog (GAH\_00449) lacking the conserved FXXDX XDGSL motif. Although previously reported archaeal cytochrome maturation pathways do not contain CcmH [37], we identified two putative CcmH proteins in the genomes of not only “*G. ahangari*” (GAH\_01092 and GAH\_01094), but also in *G. acetivorans* (GACE\_2070 and GACE\_2068)

and *F. placidus* (Ferp\_1362 and Ferp\_1364). All of these proteins contain cysteine-rich motifs consisting of LX[S,N]C[E,D,H]C but lack the LRCXXC motif characteristic of most CcmH proteins. However, they all flank a duplicate CcmF-encoding gene found only in “*G. ahangari*” (GAH\_01093), *G. acetivorans* [15], and *F. placidus* [26].

In addition to having a distinct cytochrome *c* biogenesis pathway, the iron-reducing *Archaeoglobales*, *Geoglobus* and *Ferroglobus* species, also have more *c*-type cytochromes than any other archaeon, and many of these *c*-type cytochromes have multiple heme groups [15, 18, 26]. The genome of “*G. ahangari*” contains 21 genes (Table 6) encoding putative *c*-type cytochromes, 7 of which have more than 5 heme groups; *F. placidus* has 30 *c*-type cytochromes (12 with more than 5 heme groups); and *G. acetivorans* has 16 *c*-type cytochromes (8 with more than 5 heme groups). By contrast, *Archaeoglobus* species, which do not use Fe(III)

**Table 6** Putative *c*-type cytochromes

| Gene ID:  | Annotation:   | # of heme binding motifs: | Calculated molecular weight: | TM domains: |
|-----------|---|---------------------------|------------------------------|-------------|
| GAH_00015 | Hypothetical protein  | 4                         | 58.4                         | 0           |
| GAH_00283 | Cytochrome <i>c</i> 7   | 4                         | 21.2 <sup>a</sup>            | 1           |
| GAH_00286 | Nitrate/TMAO reductases, membrane-bound tetraheme cytochrome <i>c</i> subunit | 12                        | 39.1                         | 0           |
| GAH_00301 | Putative redox-active protein (C_GCAxxG_C_C)                                  | 2                         | 31.5                         | 3           |
| GAH_00504 | Hypothetical protein  | 10                        | 54.5                         | 1           |
| GAH_00505 | Hypothetical protein  | 4                         | 26.8                         | 2           |
| GAH_00506 | Cytochrome <i>c</i> 3   | 9                         | 48.6                         | 0           |
| GAH_00507 | Cytochrome <i>c</i> 7   | 4                         | 27.4 <sup>a</sup>            | 1           |
| GAH_00508 | Hypothetical protein  | 5                         | 28.5                         | 1           |
| GAH_00510 | Hypothetical protein  | 4                         | 27.3                         | 1           |
| GAH_00817 | Seven times multi-haem cytochrome CxxCH                                       | 8                         | 53.7                         | 1           |
| GAH_01091 | Hypothetical protein  | 1                         | 11.7                         | 1           |
| GAH_01235 | Hypothetical protein  | 5                         | 21.5                         | 0           |
| GAH_01236 | Hypothetical protein  | 5                         | 22.3 <sup>b</sup>            | 0           |
| GAH_01253 | Hypothetical protein  | 4                         | 16.9                         | 0           |
| GAH_01256 | NapC/NirT cytochrome <i>c</i> family, N-terminal region                       | 10                        | 43.6 <sup>a</sup>            | 1           |
| GAH_01296 | Cytochrome <i>c</i> family protein  | 4                         | 17.2                         | 1           |
| GAH_01297 | Seven times multi-haem cytochrome CxxCH                                       | 8                         | 61.0                         | 1           |
| GAH_01306 | Class III cytochrome <i>C</i> family  | 8                         | 46.3                         | 0           |
| GAH_01534 | Hypothetical protein  | 1                         | 18.5                         | 1           |
| GAH_01700 | Hypothetical protein  | 3                         | 9.9                          | 0           |

<sup>a</sup>No signal peptide detected

<sup>b</sup>Signal peptide detected by PRED-SIGNAL

electron acceptors (Table 5), have significantly fewer *c*-type cytochromes. Within this genus, the greatest number of *c*-type cytochrome encoding genes was found in the genome of *A. veneficus*, which has 16 *c*-type cytochromes (3 with more than 5 hemes). Other species such as *A. profundus* and *A. sulfaticallidus* have only 1 monoheme *c*-type cytochrome and *A. fulgidus* has 3 *c*-type cytochromes (none of which have more than 5 heme groups).

The subcellular localization of the putative *c*-type cytochromes of “*G. ahangari*” was also investigated. The ExPASy TMPred program [42] revealed that a majority (62 %) of the *c*-type cytochromes have at least 1 transmembrane helix, consistent with their association to the cytoplasmic membrane. One of these *c*-type cytochrome proteins (GAH\_00504) was predicted to be extracellular. We also identified several *c*-type cytochromes (GAH\_01306, GAH\_00286, GAH\_01534, and GAH\_01253) with predicted sizes once in mature form (46.3, 39.1, 18.5, and 16.9 kDa, respectively) matching those reported for outer-surface heme-containing proteins required for the reduction of insoluble Fe(III) oxides, but not soluble Fe(III) citrate, by “*G. ahangari*” [14] (Table 6). Hence, these 4 *c*-type cytochromes likely function as the terminal electron carriers between the cells and the oxides.

In addition to *c*-type cytochromes, we identified other potential electron carriers such as quinones, flavoproteins, and various Fe-S proteins (*i.e.* ferredoxins). We identified a number of ubiquinone/menaquinone biosynthesis proteins in the genome of “*G. ahangari*” (Additional file 1), which could create a quinone pool in the membrane to promote electron transfer. The genome also contains a great number of Fe-S binding domain proteins and ferredoxins, which could participate in electron transfer pathways (Additional file 2). Fe-S proteins and ferredoxins were also abundant in the genome of *G. acetivorans* and *F. placidus*, which, like “*G. ahangari*”, also utilize Fe(III) respiration as their primary metabolism. Fe-S proteins and ferredoxins are regarded as some of the most ancient of electron transfer carriers [104] and also have high thermostability [105], which is critical to ensure maximum rates of electron transfer in the hot hydrothermal vent systems. Thus, the abundance of electron carrier proteins, some known to have increased thermostability, and *c*-type cytochromes, some of them localized to the outer surface, is consistent with a mechanism evolved for efficient extracellular electron transfer in hot environments.

## Conclusions

“*G. ahangari*” strain 234<sup>T</sup> is only one of three members of the *Archaeoglobales* capable of dissimilatory Fe(III) respiration. Furthermore, it is an obligate Fe(III) reducer that grows better with insoluble than soluble Fe(III) species. Consistent with this, the genome contains a large

number of *c*-type cytochromes within and on the cell surface, as well as other redox-active proteins such as thermostable ferredoxin and Fe-S proteins. The paucity of *c*-type cytochromes within non-Fe(III) respiring members of the *Archaeoglobales* (*Archaeoglobus* species) is consistent with the physiological separation between these archaea and *F. placidus*, *G. acetivorans*, and “*G. ahangari*”, which can gain energy for growth from the reduction of Fe(III) electron acceptors. Additionally, some genes required for both dissimilatory sulfate and nitrate metabolisms are absent in “*G. ahangari*” and *G. acetivorans*. This supports the physiological separation of *Geoglobus* spp. from *F. placidus*, which is capable of Fe(III)-, thiosulfate-, and nitrate respiration, and from *Archaeoglobus* species which are primarily sulfur-respiring organisms. Genomic data also support the reported physiological similarities between “*G. ahangari*” and other *Archaeoglobales* such as autotrophic growth with H<sub>2</sub> via the reductive acetyl-CoA/Wood-Ljungdahl pathway and the use of similar electron donors, including short- and long-chain fatty acids. Noteworthy is the fact that genomic evidence supports the synthesis of the methanogenic coenzyme-F<sub>420</sub> in “*G. ahangari*”, which is responsible for the characteristic fluorescence detected in all *Archaeoglobus* spp. except for “*G. ahangari*” or *F. placidus*. Hence, the genome sequence of “*G. ahangari*” provides valuable insights into its physiology and ecology as well as into the evolution of respiration within the *Archaeoglobales*.

## Taxonomic note

The initial publication [1] of the “*Geoglobus*” genus and “*Geoglobus ahangari*” species was accepted for publication with extenuating circumstances at several culture-collection agencies. Thus, upon the original publication “*G. ahangari*” strain 234<sup>T</sup> was accepted only at a single agency. In addition, the G + C mol% determined from the complete genome sequence (53.1 mol%) differs from that originally published (58.7 mol%), representing a discrepancy of over 5 mol%. This publication thus warrants an emended description of the genus *Geoglobus* and the type species, “*Geoglobus ahangari*”.

## Emended description of “*Geoglobus*” Kashefi et al.

The description of the genus “*Geoglobus*” is the one provided by Kashefi et al. [1], with the following modifications. In addition to the single monopolar flagellum, numerous curled filaments can be seen per cell [14]. The G + C content of the genomic DNA of the type species is 53.1 mol%.

## Emended description of “*Geoglobus ahangari*” Kashefi et al.

The description of the species “*Geoglobus ahangari*” is the one provided by Kashefi et al. [1, 2], with the following

modifications. The type strain is strain 234<sup>T</sup> and has been deposited at three culture collection agencies, which include the Deutsche Sammlung von Mikroorganismen und Zellkulturen (*DSM-27542*), the Japan Collection of Microorganisms (*JCM 12378*), and the American Type Culture Collection (*BAA-425*).

## Additional files

**Additional file 1: Ub iquinone and menaquinone biosynthesis proteins present in the genome of *G. ahangari*.** Ub iquinone and menaquinone biosynthesis proteins identified within the genome of *G. ahangari* strain 234<sup>T</sup>. (DOCX 16 kb)

**Additional file 2: Fe-S binding domain proteins and ferredoxins within the genome of *G. ahangari*.** Fe-S binding domain proteins and ferredoxins identified within the genome of *G. ahangari* strain 234<sup>T</sup>. (DOCX 16 kb)

## Abbreviations

SDS: Sodium dodecyl sulfate; EDTA: Ethylenediaminetetraacetic acid; TE: Tris-EDTA; EB: Elution buffer; RAST: Rapid Annotation using Subsystem Technology; IGS: Institute for Genome Sciences; IMG-ER: Integrated Microbial Genomes – Expert Review; EC: Enzyme Commission; COG: Clusters of Orthologous Group; HPLC: High performance liquid chromatography; ORB: Origin recognition box; ROK: Repressor protein, open reading frame, sugar kinase; GAPOR: Glyceraldehyde-3-phosphate:ferredoxin oxidoreductase; RuMP: Ribulose monophosphate; PRPP: 5-phosphoribosyl diphosphate; TCA: Tricarboxylic acid; Fe-S: Iron-sulfur; GS-GOGAT: Glutamine synthetase-glutamate synthase; GDH: Glutamate dehydrogenase; APS: Adenosine 5'-phosphosulfate; PAPS: 3'-phosphoadenylyl sulfate.

## Competing interests

The authors declare that they have no competing interests.

## Authors' contributions

MPM, DEH, JMR, and AC sequenced, assembled and annotated the genome. MPM, DEH, GR, JMR, and KK analyzed the data and drafted the manuscript. All authors read and approved the final manuscript.

## Acknowledgements

The authors gratefully acknowledge Tracy K. Teal at Michigan State for assistance with assembly and annotation and Abigail Vanderberg at the Center for Advanced Microscopy at Michigan State for help with scanning electron microscopy. We also acknowledge technical support provided by the Research Technology Support Facility and the Hypercomputing Center at Michigan State University, the Deep Sequencing Core Facility at the University of Massachusetts Medical School, and the Genomics Resource lab at the University of Massachusetts-Amherst. This work was supported with funds from a Strategic Partnership Grant from the MSU Foundation to GR and KK, a GAANN fellowship by the Department of Education and a DuVall Award to MPM, and a faculty grant from Western New England University to DEH and JMR.

## Author details

<sup>1</sup>Department of Microbiology and Molecular Genetics, Michigan State University, East Lansing, MI, USA. <sup>2</sup>Department of Physical and Biological Sciences, Western New England University, Springfield, MA, USA.

Received: 13 May 2015 Accepted: 7 July 2015

Published online: 09 October 2015

## References

- Kashefi K, Tor JM, Holmes DE, Gaw Van Praagh CV, Reysenbach A-L, Lovley DR. *Geoglobus ahangari* gen. nov., sp. nov., a novel hyperthermophilic archaeon capable of oxidizing organic acids and growing autotrophically on hydrogen with Fe(III) serving as the sole electron acceptor. *Int J Syst Evol Microbiol*. 2002;52:719–28. Available at: <http://ijs.sgmjournals.org/cgi/content/abstract/52/3/719>. Accessed January 13, 2015.
- Kashefi K. Hyperthermophiles: Metabolic diversity and biotechnological applications. In: Anitori RP, editor. *Extremophiles: Microbiology and Biotechnology*. Norfolk, UK: Caister Academic Press; 2012.
- Tor JM, Kashefi K, Lovley DR. Acetate oxidation coupled to Fe(III) reduction in hyperthermophilic microorganisms. *Appl Environ Microbiol*. 2001;67:1363–5. Available at: <http://www.ncbi.nlm.nih.gov/pmc/articles/PMC92735/>. Accessed January 13, 2015.
- Slobodkina G, Kolganova T, Querellou J, Bonch-Osmolovskaya E, Slobodkin A. *Geoglobus acetivorans* sp. nov., an iron(III)-reducing archaeon from a deep-sea hydrothermal vent. *Int J Syst Evol Microbiol*. 2009;59:2880–3. Available at: <http://www.ncbi.nlm.nih.gov/pubmed/19628601>. Accessed January 13, 2015.
- Hafenbradl D, Keller M, Dirmeier R, Rachel R, Roßnagel P, Burggraf S, et al. *Ferroglobus placidus* gen. nov., sp. nov., a novel hyperthermophilic archaeum that oxidizes Fe<sup>2+</sup> at neutral pH under anoxic conditions. *Arch Microbiol*. 1996;166:308–14. Available at: <http://www.ncbi.nlm.nih.gov/pubmed/8929276>. Accessed January 13, 2015.
- Beeder J, Nilsen RK, Rosnes JT, Torsvik T, Lien T. *Archaeoglobus fulgidus* isolated from hot North Sea oil field waters. *Appl Environ Microbiol*. 1994;60:1227–31. Available at: <http://aem.asm.org/content/60/4/1227.short>. Accessed January 13, 2015.
- Huber H, Jannasch H, Rachel R, Fuchs T, Stetter KO. *Archaeoglobus veneficus* sp. nov., a novel facultative chemolithoautotrophic hyperthermophilic sulfite reducer, isolated from abyssal black smokers. *Syst Appl Microbiol*. 1997;20:374–80. Available at: <http://www.sciencedirect.com/science/article/pii/S0723202097800057>. Accessed January 13, 2015.
- Mori K, Maruyama A, Urabe T, Suzuki K-I, Hanada S. *Archaeoglobus infectus* sp. nov., a novel thermophilic, chemolithoheterotrophic archaeon isolated from a deep-sea rock collected at Suiyu Seamount, Izu-Bonin Arc, western Pacific Ocean. *Int J Syst Evol Microbiol*. 2008;58:810–6. Available at: <http://www.ncbi.nlm.nih.gov/pubmed/18398174>. Accessed January 13, 2015.
- Steinsbu BO, Thorseth IH, Nakagawa S, Inagaki F, Lever MA, Engelen B, et al. *Archaeoglobus sulfatocalidus* sp. nov., a thermophilic and facultatively lithoautotrophic sulfate-reducer isolated from black rust exposed to hot ridge flank crustal fluids. *Int J Syst Evol Microbiol*. 2010;60:2745–52. Available at: <http://www.ncbi.nlm.nih.gov/pubmed/20061497>. Accessed January 13, 2015.
- Burggraf S, Jannasch HW, Nicolaus B, Stetter KO. *Archaeoglobus profundus* sp. nov., represents a new species within the sulfate-reducing archaeobacteria. *Syst Appl Microbiol*. 1990;13:24–8. Available at: <http://linkinghub.elsevier.com/retrieve/pii/S0723202011801761>. Accessed January 13, 2015.
- Lovley DR. Dissimilatory Fe(III) and Mn(IV) reduction. *Microbiol Rev*. 1991;55:259–87. Available at: <http://www.pubmedcentral.nih.gov/articlerender.fcgi?artid=372814&tool=pmcentrez&rendertype=abstract>. Accessed January 13, 2015.
- Weber KA, Achenbach LA, Coates JD. Microorganisms pumping iron: anaerobic microbial iron oxidation and reduction. *Nat Rev Microbiol*. 2006;4:752–64. Available at: <http://www.ncbi.nlm.nih.gov/pubmed/16980937>. Accessed January 13, 2015.
- Gavrilov SN, Lloyd JR, Kostrikina NA, Slobodkin AI. Fe(III) oxide reduction by a Gram-positive thermophile: Physiological mechanisms for dissimilatory reduction of poorly crystalline Fe(III) oxide by a thermophilic Gram-positive bacterium *Carboxydothemus ferrireducens*. *Geomicrobiol J*. 2012;29:804–19. Available at: <http://www.tandfonline.com/doi/abs/10.1080/01490451.2011.635755>. Accessed January 13, 2015.
- Manzella MP, Reguera G, Kashefi K. Extracellular electron transfer to Fe(III) oxides by the hyperthermophilic archaeon *Geoglobus ahangari* via a direct contact mechanism. *Appl Environ Microbiol*. 2013;79:4694–700. Available at: <http://www.ncbi.nlm.nih.gov/pubmed/23728807>. Accessed January 13, 2015.
- Mardanov AV, Slobodkina GB, Slobodkin AI, Beletsk AV, Gavrilov SN, Kublanov IV, et al. The *Geoglobus acetivorans* genome: Fe(III) reduction, acetate utilization, autotrophic growth, and degradation of aromatic compounds in a hyperthermophilic archaeon. *Appl Environ Microbiol*. 2015;81:1003–12. Available at: <http://www.ncbi.nlm.nih.gov/pubmed/25416759>. Accessed January 13, 2015.
- Wrighton KC, Thrash JC, Melnyk RA, Bigi JP, Byrne-Bailey K, Remis JP, et al. Evidence for direct electron transfer by a gram-positive bacterium isolated from a microbial fuel cell. *Appl Environ Microbiol*. 2011;77:7633–9. Available

- at: <http://www.pubmedcentral.nih.gov/articlerender.fcgi?artid=3209153&tool=pmcentrez&rendertype=abstract>. Accessed January 13, 2015.
17. Carlson HK, Iavarone AT, Gorur A, Yeo BS, Tran R, Melnyk RA, et al. Surface multiheme c-type cytochromes from *Thermincola potens* and implications for respiratory metal reduction by Gram-positive bacteria. *Proc Natl Acad Sci U S A*. 2012;109:1702–7. Available at: <http://www.pubmedcentral.nih.gov/articlerender.fcgi?artid=3277152&tool=pmcentrez&rendertype=abstract>. Accessed January 13, 2015.
  18. Smith JA, Akujkar M, Rizzo C, Leang C, Giloteaux L, Holmes DE. Mechanisms involved in Fe(III) respiration by the hyperthermophilic archaeon, *Ferroglobus placidus*. *Appl Environ Microbiol*. 2015;81:AEM.04038–14. <http://aem.asm.org/content/81/8/2735.abstract>
  19. Nevin KP, Lovley DR. Mechanisms for accessing insoluble Fe(III) oxide during dissimilatory Fe(III) reduction by *Geothrix fermentans*. *Appl Environ Microbiol*. 2002;68:2294–9. Available at: <http://aem.asm.org/cgi/content/abstract/68/5/2294>. Accessed January 13, 2015.
  20. Lovley DR, Coates JD, Blunt-Harris EL, Phillips EJ, Woodward JC. Humic substances as electron acceptors for microbial respiration. *Nature*. 1996;382:445–8. Available at: [www.nature.com/nature/journal/v382/n6590/abs/382445a0.html](http://www.nature.com/nature/journal/v382/n6590/abs/382445a0.html). Accessed January 13, 2015.
  21. Roden EE, Kappler A, Bauer I, Jiang J, Paul A, Stoesser R, et al. Extracellular electron transfer through microbial reduction of solid-phase humic substances. *Nat Geosci*. 2010;3:417–21. Available at: <http://www.nature.com/doi/10.1038/ngeo870>. Accessed January 5, 2015.
  22. Childers SE, Ciuffo S, Lovley DR. *Geobacter metallireducens* accesses insoluble Fe(III) oxide by chemotaxis. *Nature*. 2002;416:767–9. Available at: <http://www.ncbi.nlm.nih.gov/pubmed/11961561>. Accessed January 13, 2015.
  23. Lonsdale P, Becker K. Hydrothermal plumes, hot springs, and conductive heat flow in the Southern Trough of Guaymas Basin. *Earth Planet Sci Lett*. 1985;73:211–25. Available at: <http://linkinghub.elsevier.com/retrieve/pii/0012821X85900706>. Accessed January 13, 2015.
  24. Pagani I, Liolios K, Jansson J, Chen IMA, Smirnova T, Nosrat B, et al. The Genomes OnLine Database (GOLD) v. 4: Status of genomic and metagenomic projects and their associated metadata. *Nucleic Acids Res*. 2012;40:571–9.
  25. Hungate RE. The anaerobic mesophilic cellulolytic bacteria. *Bacteriol Rev*. 1950;14:1–49. Available at: <http://www.ncbi.nlm.nih.gov/pmc/articles/PMC440953/>. Accessed January 13, 2015.
  26. Anderson I, Rizzo C, Holmes DE, Lucas S, Copeland A, Lapidus A, et al. Complete genome sequence of *Ferroglobus placidus* AED112DO. *Stand Genomic Sci*. 2011;5:50–60. Available at: <http://www.pubmedcentral.nih.gov/articlerender.fcgi?artid=3236036&tool=pmcentrez&rendertype=abstract>. Accessed January 13, 2015.
  27. Bennett S. Solexa Ltd. *Pharmacogenomics*. 2004;5:433–8.
  28. Zerbinio DR, Birney E. Velvet: algorithms for de novo short read assembly using de Bruijn graphs. *Genome Res*. 2008;18:821–9. Available at: <http://www.pubmedcentral.nih.gov/articlerender.fcgi?artid=2336801&tool=pmcentrez&rendertype=abstract>. Accessed December 2, 2014.
  29. Rogers YC, Munk AC, Meincke LJ, Han CS. Closing bacterial genomic sequence gaps with adaptor-PCR. *Biotechniques*. 2005;39:31–2. 34. Available at: <http://www.ncbi.nlm.nih.gov/pubmed/16060365>. Accessed January 13, 2015.
  30. Aronesty E. ea-utils: Command-line tools for processing biological sequencing data. 2011. Available at: <https://code.google.com/p/ea-utils/>. Accessed October 16, 2014.
  31. Smeds L, Künstner A. ConDeTri—a content dependent read trimmer for Illumina data. *PLoS One*. 2011;6:e26314. Available at: <http://dx.plos.org/10.1371/journal.pone.0026314.g001>. Accessed January 13, 2015.
  32. Aziz RK, Bartels D, Best AA, DeJongh M, Disz T, Edwards RA, et al. The RAST Server: rapid annotations using subsystems technology. *BMC Genomics*. 2008;9:75. Available at: <http://www.biomedcentral.com/1471-2164/9/75>. Accessed January 4, 2015.
  33. Galens K, Orvis J, Daugherty S, Creasy HH, Angiuoli S, White O, et al. The IGS standard operating procedure for automated prokaryotic annotation. *Stand Genomic Sci*. 2011;4:244–51. Available at: <http://www.ncbi.nlm.nih.gov/pmc/articles/PMC3111993/>. Accessed January 13, 2015.
  34. Markowitz VM, Chen I-MA, Palaniappan K, Chu K, Szeto E, Pillay M, et al. IMG 4 version of the integrated microbial genomes comparative analysis system. *Nucleic Acids Res*. 2014;42:D560–7. Available at: <http://nar.oxfordjournals.org/content/42/D1/D560>. Accessed January 13, 2015.
  35. Delcher AL, Bratke KA, Powers EC, Salzberg SL. Identifying bacterial genes and endosymbiont DNA with Glimmer. *Bioinformatics*. 2007;23:673–9. Available at: <http://www.ncbi.nlm.nih.gov/pubmed/17237039>. Accessed January 13, 2015.
  36. Pati A, Ivanova NN, Mikhailova N, Ovchinnikova G, Hooper SD, Lykidis A, et al. GenePRIMP: a gene prediction improvement pipeline for prokaryotic genomes. *Nat Methods*. 2010;7:455–7. Available at: <http://www.ncbi.nlm.nih.gov/pubmed/20436475>. Accessed January 13, 2015.
  37. Allen JW, Harvat EM, Stevens JM, Ferguson SJ. A variant System I for cytochrome c biogenesis in archaea and some bacteria has a novel CcmE and no CcmH. *FEBS Lett*. 2006;580:4827–34. Available at: <http://www.ncbi.nlm.nih.gov/pubmed/16920107>. Accessed January 13, 2015.
  38. Yu NY, Wagner JR, Laird MR, Melli G, Rey S, Lo R, et al. PSORTb 3.0: improved protein subcellular localization prediction with refined localization subcategories and predictive capabilities for all prokaryotes. *Bioinformatics*. 2010;26:1608–15. Available at: <http://www.ncbi.nlm.nih.gov/pubmed/20472543>. Accessed January 13, 2015.
  39. Bagos PG, Nikolaou EP, Liakopoulos TD, Tsigiris KD. Combined prediction of Tat and Sec signal peptides with hidden Markov models. *Bioinformatics*. 2010;26:2811–7. Available at: <http://www.ncbi.nlm.nih.gov/pubmed/20847219>. Accessed January 13, 2015.
  40. Hofmann K, Stoffel W. TMbase-A database of membrane spanning protein segments. *Biol Chem Hoppe-Seyler*. 1993;35. Available at: <http://ci.niic.jp/naid/10007774832/>. Accessed January 12, 2015.
  41. Krogh A, Larsson B, von Heijne G, Sonnhammer EL. Predicting transmembrane protein topology with a hidden Markov model: application to complete genomes. *J Mol Biol*. 2001;305:567–80. Available at: <http://www.ncbi.nlm.nih.gov/pubmed/11152613>. Accessed July 9, 2014.
  42. Wilkins MR, Gasteiger E, Bairoch A, Sanchez JC, Williams KL, Appel RD, et al. Protein identification and analysis tools in the ExPASy server. *Methods Mol Biol*. 1999;112:531–52. Available at: <http://link.springer.com/10.1385/1-59259-890-0:571>. Accessed January 13, 2015.
  43. Klenk HP, Clayton RA, Tomb JF, White O, Nelson KE, Ketchum KA, et al. The complete genome sequence of the hyperthermophilic, sulphate-reducing archaeon *Archaeoglobus fulgidus*. *Nature*. 1997;390:364–70. Available at: <http://www.ncbi.nlm.nih.gov/pubmed/9389475>. Accessed January 13, 2015.
  44. Von Jan M, Lapidus A, Del Rio TG, Copeland A, Tice H, Cheng J-F, et al. Complete genome sequence of *Archaeoglobus profundus* type strain (AV18). *Stand Genomic Sci*. 2010;2:327–46. Available at: <http://www.pubmedcentral.nih.gov/articlerender.fcgi?artid=3035285&tool=pmcentrez&rendertype=abstract>. Accessed January 13, 2015.
  45. Stokke R, Hocking WP, Steinsbu BO, Steen IH. Complete genome sequence of the thermophilic and facultatively chemolithoautotrophic sulfate reducer *Archaeoglobus sulfatocalidus* strain PM70-1T. *Genome Announc*. 2013;1:4–5. Available at: <http://www.ncbi.nlm.nih.gov/pmc/articles/PMC3703591>. Accessed January 13, 2015.
  46. Grabowski B, Kelman Z. Archeal DNA replication: eukaryal proteins in a bacterial context. *Annu Rev Microbiol*. 2003;57:487–516. Available at: <http://www.ncbi.nlm.nih.gov/pubmed/14527289>. Accessed January 13, 2015.
  47. Wu Z, Liu J, Yang H, Xiang H. DNA replication origins in archaea. *Front Microbiol*. 2014;5:179. Available at: <http://www.pubmedcentral.nih.gov/articlerender.fcgi?artid=4010727&tool=pmcentrez&rendertype=abstract>. Accessed January 13, 2015.
  48. Gao F, Zhang C-T. DoriC: a database of oriC regions in bacterial genomes. *Bioinformatics*. 2007;23:1866–7. Available at: <http://www.ncbi.nlm.nih.gov/pubmed/17496319>. Accessed January 13, 2015.
  49. Wu Z, Liu J, Yang H, Liu H, Xiang H. Multiple replication origins with diverse control mechanisms in *Haloarcula hispanica*. *Nucleic Acids Res*. 2014;42:2282–94. Available at: <http://www.pubmedcentral.nih.gov/articlerender.fcgi?artid=3936714&tool=pmcentrez&rendertype=abstract>. Accessed January 13, 2015.
  50. Wood HG. Life with CO or CO<sub>2</sub> and H<sub>2</sub> as a source of carbon and energy. *FASEB J*. 1991;5:156–63. Available at: <http://www.ncbi.nlm.nih.gov/pubmed/1900793>. Accessed January 13, 2015.
  51. Drake HL, Gössner AS, Daniel SL. Old acetogens, new light. *Ann N Y Acad Sci*. 2008;1125:100–28. Available at: <http://www.ncbi.nlm.nih.gov/pubmed/18378590>. Accessed December 26, 2014.
  52. Ragsdale SW. Enzymology of the Wood-Ljungdahl pathway of acetogenesis. *Ann N Y Acad Sci*. 2008;1125:129–36. Available at: <http://www.ncbi.nlm.nih.gov/pubmed/18378591>. Accessed December 28, 2014.

53. Ljungdahl LG. The autotrophic pathway of acetate synthesis in acetogenic bacteria. *Annu Rev Microbiol.* 1986;40:415–50. Available at: <http://www.ncbi.nlm.nih.gov/pubmed/3096193>. Accessed January 13, 2015.
54. Berg IA, Kockelkorn D, Ramos-Vera WH, Say RF, Zarzycki J, Hügler M, et al. Autotrophic carbon fixation in archaea. *Nat Rev Microbiol.* 2010;8:447–60. Available at: <http://www.ncbi.nlm.nih.gov/pubmed/20453874>. Accessed January 13, 2015.
55. Vormolt J, Kunow J, Stetter KO, Thauer RK. Enzymes and coenzymes of the carbon monoxide dehydrogenase pathway for autotrophic CO<sub>2</sub> fixation in *Archaeoglobus lithotrophicus* and the lack of carbon monoxide dehydrogenase in the heterotrophic *A. profundus*. *Arch Microbiol.* 1995;163:112–8. Available at: <http://link.springer.com/article/10.1007%2FBF00381784>. Accessed January 13, 2015.
56. Estelmann S, Ramos-Vera WH, Gad'on N, Huber H, Berg IA, Fuchs G. Carbon dioxide fixation in *Archaeoglobus lithotrophicus*: are there multiple autotrophic pathways? *FEMS Microbiol Lett.* 2011;319:65–72. Available at: <http://www.ncbi.nlm.nih.gov/pubmed/21410513>. Accessed October 22, 2014.
57. Vorholt J, Hafenbradl D, Stetter K, Thauer R. Pathways of autotrophic CO<sub>2</sub> fixation and of dissimilatory nitrate reduction to N<sub>2</sub>O in *Ferroglobus placidus*. *Arch Microbiol.* 1997;167:19–23. Available at: <http://www.ncbi.nlm.nih.gov/pubmed/9000337>. Accessed January 13, 2015.
58. Möller-Zinkhan D, Börner G, Thauer RK. Function of methanofuran, tetrahydromethanopterin, and coenzyme F<sub>420</sub> in *Archaeoglobus fulgidus*. *Arch Microbiol.* 1989;152:362–8. Available at: <http://link.springer.com/article/10.1007/BF00249070?no-access=true>. Accessed January 13, 2015.
59. Wood H. The acetyl-CoA pathway of autotrophic growth. *FEMS Microbiol Lett.* 1986;39:345–62. Available at: <http://www.sciencedirect.com/science/article/pii/0378109786900224>. Accessed January 13, 2015.
60. Kunow J, Schwörer B, Setzke E, Thauer RK. Si-face stereospecificity at C5 of coenzyme F420 for F420-dependent N5, N10-methylenetetrahydromethanopterin dehydrogenase, F420-dependent N5, N10-methylenetetrahydromethanopterin reductase and F420H2: dimethylnaphthoquinone oxidoreductase. *Eur J Biochem.* 1993;214:641–6. Available at: <http://www.ncbi.nlm.nih.gov/pubmed/8319675>. Accessed January 13, 2015.
61. Möller-Zinkhan D, Thauer RK. Anaerobic lactate oxidation to 3 CO<sub>2</sub> by *Archaeoglobus fulgidus* via the carbon monoxide dehydrogenase pathway: demonstration of the acetyl-CoA carbon-carbon cleavage reaction in cell extracts. *Arch Microbiol.* 1990;153:215–8. Available at: <http://link.springer.com/article/10.1007/BF00249070?no-access=true>. Accessed January 13, 2015.
62. Schmitz RA, Linder D, Stetter KO, Thauer RK. N5, N10-Methylenetetrahydromethanopterin reductase (coenzyme F420-dependent) and formylmethanofuran dehydrogenase from the hyperthermophile *Archaeoglobus fulgidus*. *Arch Microbiol.* 1991;156:427–34. Available at: <http://link.springer.com/article/10.1007/BF00248722>. Accessed January 13, 2015.
63. Coppi MV. The hydrogenases of *Geobacter sulfurreducens*: a comparative genomic perspective. *Microbiology.* 2005;151:1239–54. Available at: <http://www.ncbi.nlm.nih.gov/pubmed/15817791>. Accessed April 28, 2014.
64. Deppenmeier U. Redox-driven proton translocation in methanogenic archaea. *Cell Mol Life Sci.* 2002;59:1513–33.
65. Graham DE, Xu H, White RH. Identification of the 7,8-didemethyl-8-hydroxy-5-deazariboflavin synthase required for coenzyme F<sub>420</sub> biosynthesis. *Arch Microbiol.* 2003;180:455–64. Available at: <http://www.ncbi.nlm.nih.gov/pubmed/14593448>. Accessed December 15, 2014.
66. Bräsen C, Esser D, Rauch B, Siebers B. Carbohydrate metabolism in Archaea: current insights into unusual enzymes and pathways and their regulation. *Microbiol Mol Biol Rev.* 2014;78:89–175. Available at: <http://www.ncbi.nlm.nih.gov/pubmed/24600042>.
67. Hansen T, Schönheit P. ADP-dependent 6-phosphofructokinase, an extremely thermophilic, non-allosteric enzyme from the hyperthermophilic, sulfate-reducing archaeon *Archaeoglobus fulgidus* strain 7324. *Extremophiles.* 2004;8:29–35.
68. Hansen T, Schönheit P. Purification and properties of the first-identified, archaeal, ATP-dependent 6-phosphofructokinase, an extremely thermophilic non-allosteric enzyme, from the hyperthermophile *Desulfurococcus amylolyticus*. *Arch Microbiol.* 2000;173:103–9.
69. Hansen T, Schönheit P. Sequence, expression, and characterization of the first archaeal ATP-dependent 6-phosphofructokinase, a non-allosteric enzyme related to the phosphofructokinase-B sugar kinase family, from the hyperthermophilic crenarchaeote *Aeropyrum pernix*. *Arch Microbiol.* 2002;177:62–9.
70. Say RF, Fuchs G. Fructose 1,6-bisphosphate aldolase/phosphatase may be an ancestral gluconeogenic enzyme. *Nature.* 2010;464:1077–81. Available at: <http://www.ncbi.nlm.nih.gov/pubmed/20348906>. Accessed January 13, 2015.
71. Johnsen U, Schönheit P. Characterization of cofactor-dependent and cofactor-independent phosphoglycerate mutases from Archaea. *Extremophiles.* 2007;11:647–57.
72. Johnsen U, Hansen T, Schönheit P. Comparative analysis of pyruvate kinases from the hyperthermophilic archaea *Archaeoglobus fulgidus*, *Aeropyrum pernix*, and *Pyrobaculum aerophilum* and the hyperthermophilic bacterium *Thermotoga maritima*: Unusual regulatory properties in hyperthermophilic archaea. *J Biol Chem.* 2003;278:25417–27.
73. Orita I, Sato T, Yurimoto H, Kato N, Atomi H, Imanaka T, et al. The ribulose monophosphate pathway substitutes for the missing pentose phosphate pathway in the archaeon *Thermococcus kodakaraensis*. *J Bacteriol.* 2006;188:4698–704. Available at: <http://www.ncbi.nlm.nih.gov/pubmed/16788179>. Accessed January 7, 2015.
74. Makarova KS, Koonin EV. Filling a gap in the central metabolism of archaea: prediction of a novel aconitase by comparative-genomic analysis. *FEMS Microbiol Lett.* 2003;227:17–23. Available at: <http://www.ncbi.nlm.nih.gov/pubmed/14568143>.
75. Zwolinski, Harris RF, Hickey WJ. Microbial consortia involved in the anaerobic degradation of hydrocarbons. *Biodegradation.* 2000;11:141–58. Available at: <http://www.ncbi.nlm.nih.gov/pubmed/11440241>. Accessed January 13, 2015.
76. So CM, Phelps CD, Young LY. Anaerobic transformation of alkanes to fatty acids by a sulfate-reducing bacterium, Strain Hxd3. *Appl Environ Microbiol.* 2003;69:3892–900. Available at: <http://www.ncbi.nlm.nih.gov/pmc/articles/PMC165127/>. Accessed January 13, 2015.
77. Atlas RM. Microbial degradation of petroleum hydrocarbons: an environmental perspective. *Microbiol Rev.* 1981;45:180–209. Available at: <http://www.ncbi.nlm.nih.gov/pmc/articles/pmc281502/>. Accessed January 13, 2015.
78. Mbandinga SM, Li K-P, Zhou L, Wang L-Y, Yang S-Z, Liu J-F, et al. Analysis of alkane-dependent methanogenic community derived from production water of a high-temperature petroleum reservoir. *Appl Microbiol Biotechnol.* 2012;96:531–42. Available at: <http://www.ncbi.nlm.nih.gov/pubmed/22249716>. Accessed December 13, 2014.
79. Tor JM, Lovley DR. Anaerobic degradation of aromatic compounds coupled to Fe(III) reduction by *Ferroglobus placidus*. *Environ Microbiol.* 2001;3:281–7. Available at: <http://www.ncbi.nlm.nih.gov/pubmed/11359514>. Accessed January 13, 2015.
80. Holmes DE, Rizzo C, Smith JA, Lovley DR. Genome-scale analysis of anaerobic benzoate and phenol metabolism in the hyperthermophilic archaeon *Ferroglobus placidus*. *ISME J.* 2012;6:146–57. Available at: <http://www.ncbi.nlm.nih.gov/pubmed/21776029>. Accessed January 13, 2015.
81. Holmes DE, Rizzo C, Smith JA, Lovley DR. Anaerobic oxidation of benzene by the hyperthermophilic archaeon *Ferroglobus placidus*. *Appl Environ Microbiol.* 2011;77:5926–33. Available at: <http://www.ncbi.nlm.nih.gov/pubmed/21742914>. Accessed January 13, 2015.
82. Khelifi N, Grossi V, Hamdi M, Dolla A, Tholozan J-L, Ollivier B, et al. Anaerobic oxidation of fatty acids and alkenes by the hyperthermophilic sulfate-reducing archaeon *Archaeoglobus fulgidus*. *Appl Environ Microbiol.* 2010;76:3057–60. Available at: <http://www.ncbi.nlm.nih.gov/pubmed/20305028>. Accessed January 13, 2015.
83. Khelifi N, Amin Ali O, Roche P, Grossi V, Brochier-Armanet C, Valette O, et al. Anaerobic oxidation of long-chain n-alkanes by the hyperthermophilic sulfate-reducing archaeon, *Archaeoglobus fulgidus*. *ISME J.* 2014;8:3057–60. Available at: <http://www.ncbi.nlm.nih.gov/pubmed/24763368>. Accessed January 13, 2015.
84. Johnson HA, Pelletier DA, Spormann AM. Isolation and characterization of anaerobic ethylbenzene dehydrogenase, a novel Mo-Fe-S enzyme. *J Bacteriol.* 2001;183:4536–42. Available at: <http://www.ncbi.nlm.nih.gov/pubmed/11443088>.
85. Rabus R, Kube M, Heider J, Beck A, Heitmann K, Widdel F, et al. The genome sequence of an anaerobic aromatic-degrading denitrifying bacterium, strain EbN1. *Arch Microbiol.* 2005;183:27–36. Available at: <http://www.ncbi.nlm.nih.gov/pubmed/15551059>. Accessed January 13, 2015.
86. Cabello P, Roldán MD, Moreno-Vivián C. Nitrate reduction and the nitrogen cycle in archaea. *Microbiology.* 2004;150:3527–46. Available at: <http://www.ncbi.nlm.nih.gov/pubmed/15528644>. Accessed January 13, 2015.

87. Mehta MP, Butterfield DA, Baross JA. Phylogenetic diversity of nitrogenase (nifH) genes in deep-sea and hydrothermal vent environments of the Juan de Fuca Ridge. *Appl Environ Microbiol.* 2003;69:960–70. Available at: <http://www.ncbi.nlm.nih.gov/pubmed/12571018>. Accessed January 13, 2015.
88. Charlou JL, Donval JP, Douville E, Jean-Baptiste P, Radford-Knoery J, Fouquet Y, et al. Compared geochemical signatures and the evolution of Menez Gwen (37°50'N) and Lucky Strike (37°17'N) hydrothermal fluids, south of the Azores Triple Junction on the Mid-Atlantic Ridge. *Chem Geol.* 2000;171:49–75. Available at: <http://linkinghub.elsevier.com/retrieve/pii/S0009254100002448>. Accessed January 13, 2015.
89. Karl DM, Taylor GT, Novitsky JA, Jannasch HW, Wirsén CO, Pace NR, et al. A microbiological study of Guaymas Basin high temperature hydrothermal vents. *Deep Sea Res A Oceanogr Res Pap.* 1988;35:777–91. Available at: <http://linkinghub.elsevier.com/retrieve/pii/0198014988900301>. Accessed January 13, 2015.
90. Canfield DE, Kristensen E, Thamdrup B. Aquatic geomicrobiology. *Adv Mar Biol.* 2005;48:1–599. Available at: <http://www.ncbi.nlm.nih.gov/pubmed/15797449>. Accessed January 13, 2015.
91. Bick JA, Leustek T. Plant sulfur metabolism — the reduction of sulfate to sulfite. *Curr Opin Plant Biol.* 1998;1:240–4. Available at: <http://linkinghub.elsevier.com/retrieve/pii/S1369526698801118>. Accessed January 13, 2015.
92. Peck HD. Enzymatic basis for assimilatory and dissimilatory sulfate reduction. *J Bacteriol.* 1961;82:933–9. Available at: <http://www.ncbi.nlm.nih.gov/pubmed/14484818>. Accessed January 13, 2015.
93. Postgate J. Sulphate reduction by bacteria. *Annu Rev Microbiol.* 1959;13:505–20. Available at: <http://www.annualreviews.org/doi/abs/10.1146/annurev.mi.13.100159.002445?journalCode=micro>. Accessed January 13, 2015.
94. Fritz G, Einsle O, Rudolf M, Schiffer A, Kroneck PMH. Key bacterial multi-centered metal enzymes involved in nitrate and sulfate respiration. *J Mol Microbiol Biotechnol.* 2005;10:223–33. Available at: <http://www.ncbi.nlm.nih.gov/pubmed/16645317>. Accessed October 28, 2014.
95. Hansen TA. Metabolism of sulfate-reducing prokaryotes. *Antonie Van Leeuwenhoek.* 1994;66:165–85. Available at: <http://www.ncbi.nlm.nih.gov/pubmed/7747930>. Accessed January 13, 2015.
96. Parey K, Fritz G, Ermler U, Kroneck PMH. Conserving energy with sulfate around 100 °C—structure and mechanism of key metal enzymes in hyperthermophilic *Archaeoglobus fulgidus*. *Metallomics.* 2013;5:302–17. Available at: <http://www.ncbi.nlm.nih.gov/pubmed/23324858>. Accessed January 13, 2015.
97. Jarrell KF, Albers S-V. The archaellum: an old motility structure with a new name. *Trends Microbiol.* 2012;20:307–12. Available at: <http://www.ncbi.nlm.nih.gov/pubmed/22613456>. Accessed February 21, 2014.
98. Desmond E, Brochier-Amanet C, Gribaldo S. Phylogenomics of the archaeal flagellum: rare horizontal gene transfer in a unique motility structure. *BMC Evol Biol.* 2007;7:106. Available at: <http://www.biomedcentral.com/1471-2148/7/106>. Accessed January 13, 2015.
99. Voisin S, Houliston RS, Kelly J, Brisson J-R, Watson D, Bardy SL, et al. Identification and characterization of the unique N-linked glycan common to the flagellins and S-layer glycoprotein of *Methanococcus voltae*. *J Biol Chem.* 2005;280:16586–93. Available at: <http://www.ncbi.nlm.nih.gov/pubmed/15723834>. Accessed January 13, 2015.
100. Eichler J. Extreme sweetness: protein glycosylation in archaea. *Nat Rev Microbiol.* 2013;11:151–6. Available at: <http://www.nature.com/nrmicro/journal/v11/n3/full/nrmicro2957.html>. Accessed January 13, 2015.
101. Jørgensen BB, Zawacki LX, Jannasch HW. Thermophilic bacterial sulfate reduction in deep-sea sediments at the Guaymas Basin hydrothermal vent site (Gulf of California). *Deep Sea Res A Oceanogr Res Pap.* 1990;37:695–710. Available at: <http://linkinghub.elsevier.com/retrieve/pii/019801499090099H>. Accessed December 9, 2014.
102. Esquivel RN, Xu R, Pohlschroder M. Novel archaeal adhesion pilins with a conserved N terminus. *J Bacteriol.* 2013;195:3808–18. Available at: <http://www.ncbi.nlm.nih.gov/pubmed/23794623>. Accessed December 16, 2014.
103. Shi L, Richardson DJ, Wang Z, Kerisit SN, Rosso KM, Zachara JM, et al. The roles of outer membrane cytochromes of *Shewanella* and *Geobacter* in extracellular electron transfer. *Environ Microbiol Rep.* 2009;1:220–7. Available at: <http://onlinelibrary.wiley.com/doi/10.1111/j.1758-2229.2009.00035.x/abstract>.
104. Wächtershäuser G. Before enzymes and templates: theory of surface metabolism. *Microbiol Rev.* 1988;52:452–84. Available at: <http://www.ncbi.nlm.nih.gov/pmc/articles/PMC373159/>. Accessed January 8, 2015.
105. Aono S, Bryant FO, Adams MW. A novel and remarkably thermostable ferredoxin from the hyperthermophilic archaeobacterium *Pyrococcus furiosus*. *J Bacteriol.* 1989;171:3433–9. Available at: <http://www.ncbi.nlm.nih.gov/pubmed/2542225>. Accessed January 7, 2015.
106. Field D. The minimum information about a genome sequence (MIGS) specification. *Nat Biotechnol.* 2008;26:541–7. Available at: <http://www.ncbi.nlm.nih.gov/pubmed/18464787>.
107. Woese CR, Kandler O, Wheelis ML. Towards a natural system of organisms: proposal for the domains Archaea, Bacteria, and Eucarya. *Proc Natl Acad Sci U S A.* 1990;87:4576–9.
108. Garrity GM, Holt JG, Whitman WB, Keswani J, Boone DR, Koga Y, et al. Phylum All. Euryarchaeota phyl. nov. In: *Bergey's Manual® of Systematic Bacteriology*; 2001:211–355. Available at: [http://link.springer.com/chapter/10.1007%2F978-0-387-21609-6\\_17](http://link.springer.com/chapter/10.1007%2F978-0-387-21609-6_17).
109. Garrity GM, Holt JG. Class VI. Archaeoglobi class. nov. 2nd ed. (Garrity GM, Boone DR, Castenholz RW, eds.). New York: Springer; 2001.
110. Huber H, Stetter KO. Order I. Archaeoglobales ord. nov. 2nd ed. (Garrity GM, Boone DR, Castenholz RW, eds.). New York: Springer; 2001.
111. Huber H, Stetter KO. Family I. Archaeoglobaceae fam. nov. Stetter 1989, 2216. 2nd ed. (Garrity GM, Boone DR, Castenholz RW, eds.). New York: Springer; 2001.
112. Ashburner M, Ball CA, Blake JA, Botstein D, Butler H, Cherry JM, et al. Gene ontology: tool for the unification of biology. The Gene Ontology Consortium. *Nat Genet.* 2000;25:25–9.

**Submit your next manuscript to BioMed Central and take full advantage of:**

- Convenient online submission
- Thorough peer review
- No space constraints or color figure charges
- Immediate publication on acceptance
- Inclusion in PubMed, CAS, Scopus and Google Scholar
- Research which is freely available for redistribution

Submit your manuscript at  
[www.biomedcentral.com/submit](http://www.biomedcentral.com/submit)

